

AD_____

Award Number: DAMD17-01-1-0777

TITLE: Fundamental Patterns Underlying Neurotoxicity Revealed by
DNA Microarray Expression Profiling

PRINCIPAL INVESTIGATOR: Karen L. O'Malley, Ph.D.

CONTRACTING ORGANIZATION: Washington University School of Medicine
St. Louis, Missouri 63110-1093

REPORT DATE: September 2003

TYPE OF REPORT: Annual

PREPARED FOR: U.S. Army Medical Research and Materiel Command
Fort Detrick, Maryland 21702-5012

DISTRIBUTION STATEMENT: Approved for Public Release;
Distribution Unlimited

The views, opinions and/or findings contained in this report are those of the author(s) and should not be construed as an official Department of the Army position, policy or decision unless so designated by other documentation.

20040903 126

REPORT DOCUMENTATION PAGEForm Approved
OMB No. 074-0188

Public reporting burden for this collection of information is estimated to average 1 hour per response, including the time for reviewing instructions, searching existing data sources, gathering and maintaining the data needed, and completing and reviewing this collection of information. Send comments regarding this burden estimate or any other aspect of this collection of information, including suggestions for reducing this burden to Washington Headquarters Services, Directorate for Information Operations and Reports, 1215 Jefferson Davis Highway, Suite 1204, Arlington, VA 22202-4302, and to the Office of Management and Budget, Paperwork Reduction Project (0704-0188), Washington, DC 20503

1. AGENCY USE ONLY
(Leave blank)**2. REPORT DATE**

September 2003

3. REPORT TYPE AND DATES COVERED

Annual (1 Sep 2002 - 31 Aug 2003)

4. TITLE AND SUBTITLEFundamental Patterns Underlying Neurotoxicity Revealed by
DNA Microarray Expression Profiling**5. FUNDING NUMBERS**

DAMD17-01-1-0777

6. AUTHOR(S)

Karen L. O'Malley, Ph.D.

7. PERFORMING ORGANIZATION NAME(S) AND ADDRESS(ES)Washington University School of Medicine
St. Louis, Missouri 63110-1093**8. PERFORMING ORGANIZATION
REPORT NUMBER****E-Mail:** omalleyk@pcg.wustl.edu**9. SPONSORING / MONITORING****AGENCY NAME(S) AND ADDRESS(ES)**U.S. Army Medical Research and Materiel Command
Fort Detrick, Maryland 21702-5012**10. SPONSORING / MONITORING
AGENCY REPORT NUMBER****11. SUPPLEMENTARY NOTES**

Original contains color plates: All DTIC reproductions will be in black and white.

12a. DISTRIBUTION / AVAILABILITY STATEMENT

Approved for Public Release; Distribution Unlimited

12b. DISTRIBUTION CODE**13. ABSTRACT (Maximum 200 Words)**

The selective neurotoxins 1-methyl-4-phenylpyridinium (MPP⁺) and 6-hydroxydopamine (6-OHDA) have been widely used to generate animal models of Parkinson's disease (PD). To understand the genetic events associated with these neurotoxins, microarray technology served to monitor differences in gene expression patterns in normal versus pathological conditions. Microarray analysis of RNA isolated from toxin treated samples revealed that the stress induced transcription factor CHOP was dramatically up regulated by both toxins. 6-OHDA also induced a large number of genes involved in endoplasmic reticulum (ER) stress and unfolded protein response (UPR) such as ER chaperones and elements of the ubiquitin-proteasome system. RT-PCR, Western blotting, and immunocytochemical approaches were used to quantify and temporarily order the UPR pathways involved in neurotoxin-induced cell death. 6-OHDA, but not MPP⁺, significantly increased hallmarks of UPR such as BiP, c-jun, and processed Xbp1 mRNA. Both toxins increased the phosphorylation of UPR proteins, PERK and eIF2 α , but only 6-OHDA increased phosphorylation of c-jun. Thus, 6-OHDA triggers multiple pathways associated with UPR, whereas MPP⁺ exhibits a more restricted response. 6-OHDA induced similar responses in primary dopaminergic neurons. These experiments will help clarify the molecular mechanisms associated with 6-OHDA and MPP⁺ toxicity and might aid in developing novel therapeutic avenues relevant to PD.

14. SUBJECT TERMSMPP⁺; 6-OHDA; Neurotoxicity; Gene expression profiling; DNA
microarray**15. NUMBER OF PAGES**

32

16. PRICE CODE**17. SECURITY CLASSIFICATION
OF REPORT**

Unclassified

**18. SECURITY CLASSIFICATION
OF THIS PAGE**

Unclassified

**19. SECURITY CLASSIFICATION
OF ABSTRACT**

Unclassified

20. LIMITATION OF ABSTRACT

Unlimited

NSN 7540-01-280-5500

Standard Form 298 (Rev. 2-89)
Prescribed by ANSI Std. Z39-18
298-102

Table of Contents

Cover.....	1
SF 298.....	2
Table of Contents.....	3
Introduction.....	4
Body.....	4
Key Research Accomplishments.....	9
Reportable Outcomes.....	9
Conclusions.....	9
References.....	10
Appendices.....	12

Introduction

Accumulating evidence suggests that Endoplasmic Reticulum (ER) stress/Unfolded Protein Response (UPR)-mediated cell death plays a role in Parkinson's disease (PD) based on genetic, pharmacological and environmental factors. For example, α -synuclein, the major component of Lewy bodies (Spillantini et al., 1997), is associated with protein aggregation and proteosomal dysfunction (Betarbet et al., 2002). Additionally, Parkin, the protein associated with autosomal recessive juvenile Parkinsonism (AR-JP; Kitada et al., 1998) has been shown to be an E3 ubiquitin-protein ligase (Shimura et al., 2000). Reports that Parkin substrates misfold, aggregate, and trigger ER stress/UPR suggest that Parkin activity prevents the accumulation of misfolded proteins (Imai et al., 2001; Tsai et al., 2003). The role of proteosomal impairment has been further emphasized by recent findings that pharmacological inhibition of proteasome function leads to selective degeneration of dopaminergic neurons in culture (McNaught et al., 2002a) as well as in vivo (McNaught et al., 2002b). Finally, recent studies from this lab (Holtz and O'Malley, 2003) as well as others (Ryu et al., 2002) have linked oxidative stress, a well-documented factor in PD, with ER stress/UPR as well.

Beginning with a functional genomics approach to identify transcriptional alterations in a well-characterized model of 6-OHDA and MPP⁺ toxicity, studies conducted under the auspices of this grant identified numerous changes in genes associated with ER stress/UPR (Holtz and O'Malley, 2003). Reverse transcription/PCR amplification, western blots and immunocytochemistry were used to verify changes in selected subsets of differentially regulated transcripts. Selected transcripts were also tested for toxin-induced changes in primary cultured dopaminergic neurons. Just as studies in other model systems have uncovered novel signaling pathways, these experiments are also revealing unanticipated pathways that contribute to MPP⁺ and 6-OHDA neurotoxicity. Taken together, these and other findings support the theory that proteosomal dysfunction with ensuing ER stress/UPR contribute to PD.

Body

A. Does the neurotoxin MPP⁺ differentially regulate sets of genes?

To test the hypothesis that MPP⁺ alters gene transcription as part of its neurotoxic program, a time course study using cycloheximide to block MPP⁺ toxicity, was performed as previously described. Briefly, cells were treated with 50 μ M MPP⁺ with 10 μ M cycloheximide being added for varying periods of time. The point at which about 50 % of the cells were rescued by blocking protein synthesis, 9 hours following MPP⁺ treatment, was chosen as the best time point at which to harvest RNA.

In consultation with experts from our onsite Affymetrix gene chip core facility, we subsequently designed our experiments such that a minimum of 3 separate experiments were performed in which cells were treated with MPP⁺ for 9 hours and then harvested for RNA preparation at that time point. Cell death was verified in each case by independent experiments done on sibling cultures. RNAs from all three experiments were pooled to form an RNA resource that would minimize experimental variation.

RNA sample preparation was done according to protocols devised by Affymetrix to achieve the best results, particularly for mammalian cells. Specific details of preparation and hybridization

were described previously and are detailed in the attached manuscript (Holtz and O'Malley, 2003).

The data obtained for MPP⁺ are compiled values from three separate experiments done in triplicate as described above. The expression level of each probe set was plotted to determine the reproducibility of the array-based hybridization signals and to compare gene expression levels by MN9D cells treated with and without MPP⁺. The ratio of gene intensity in toxin-treated cells to that in control samples was used to represent the toxin-mediated induction. The reciprocal ratio represented repression. Genes were considered up or down-regulated if the fold change was at least 2.0 in individual experiments as well as in averaged, triplicated experiments. These limits are in general agreement with most gene chip experiments.

Out of the approximately 12,000 genes and ESTs represented on the MG-U74Av2 GeneChip, 4,304 (~35% of total) were defined as "present" by the microarray analysis software for MPP⁺-treated samples. Transcripts were subsequently grouped by individual toxin treatment or by both 6-OHDA and MPP⁺. As indicated in Table 1, only 59 transcripts increased in response to MPP⁺. Results for decreasing transcripts were somewhat less (Table 2). Both neurotoxins induced a number of the same transcripts, with 43 of the 59 transcripts induced by MPP⁺ also induced by 6-OHDA (Table 3). These included genes involved in cell cycle and/or differentiation, signaling, stress, and transcription factors, indicating possible common cell death mechanisms. The most highly induced transcript in response to either treatment was that to the stress protein CHOP/Gadd153. These results support previous findings showing that MPP⁺ and 6-OHDA promote distinct yet overlapping programs of cell death.

As described in more detail below (C; Holtz and O'Malley, 2003), MPP⁺ appears to specifically induce one arm of the ER stress/Unfolded Protein Response (UPR)-mediated cell death pathway. Interestingly, time course data generated for pathway constituents indicated that between 1-3 hours something occurs in MPP⁺ treated cells that leads to a decline in the ER stress/UPR markers (see Figs 4-5, attached publication Holtz and O'Malley, 2003). As part of the original research proposal and in order to determine whether transcriptional changes are mediating this effect, we have now prepared MPP⁺-treated RNA at 1 and 6 hours exactly as previously described. Aliquots of the pooled RNA from these experiments are queued at the Washington University School of Medicine DNA array facility. We should receive these new data in the next few weeks. The additional information will allow us to analyze MPP⁺-mediated transcriptional changes in significantly more depth than our original single time point has allowed.

B. Does the neurotoxin 6-OHDA differentially regulate sets of genes?

To test the hypothesis that 6-OHDA neurotoxicity alters fundamental patterns of gene expression, experiments were conducted exactly as described above for MPP⁺. Out of the approximately 12,000 genes and ESTs represented on the GeneChip, 4,580 (~37% of total) were defined as present for 6-OHDA-treated samples. Notably, 6-OHDA treatment affected almost three times as many transcripts as MPP⁺. Specifically, 157 transcripts increased in response to 6-OHDA (Table 4) and 41 decreased (Table 5). As described, the most highly induced transcript in response to either treatment was that to CHOP. 6-OHDA also induced a large number of transcripts that were unchanged by MPP⁺ treatment, including molecular chaperones and other genes involved in protein folding, trafficking, and the ubiquitin-proteasome pathway (Table 3).

Because 6-OHDA appeared to induce apoptosis in this model system as well as in primary cultured neurons (Oh et al., 1995; Lotharius et al., 1999; Choi et al., 1999), we anticipated the identification of functional clusters of neurotoxin-responsive genes that would overlap with apoptotic patterns observed in other models. Surprisingly, however, many of the genes that were up regulated were again members of the ER stress/UPR cell death pathway. Indeed, Chop induction was even more pronounced in 6-OHDA treated cells than in MPP⁺ Table 3).

Currently, we have also prepared RNA from MN9D cells treated with 6-OHDA for 1 and 6 hours. These samples, like those for the MPP⁺-treated RNA pools are awaiting processing at our DNA array facility. The wealth of new information being generated with further our attempts to order and delineate 6-OHDA mediated cell death pathways.

C. Verification in MN9D Cells

To verify induction or repression by an independent method, a subset of the most interesting differentially regulated genes were examined by RT/PCR, Western blotting and immunocytochemical approaches. These methodologies allowed us to quantitate and temporally order the ER stress/UPR pathways involved in neurotoxin-induced cell death. As detailed in the attached publication (Holtz and O'Malley, 2003), 6-OHDA, but not MPP⁺, significantly increased hallmarks of UPR such as BiP, c-jun, and processed Xbp1 mRNA. Both toxins increased the phosphorylation of UPR proteins, PERK and eIF2 α , but only 6-OHDA increased phosphorylation of c-jun. Thus, 6-OHDA is capable of triggering multiple pathways associated with UPR, whereas MPP⁺ exhibits a more restricted response. These results allowed us to derive a working model (Fig. 1) from which we can test further hypotheses.

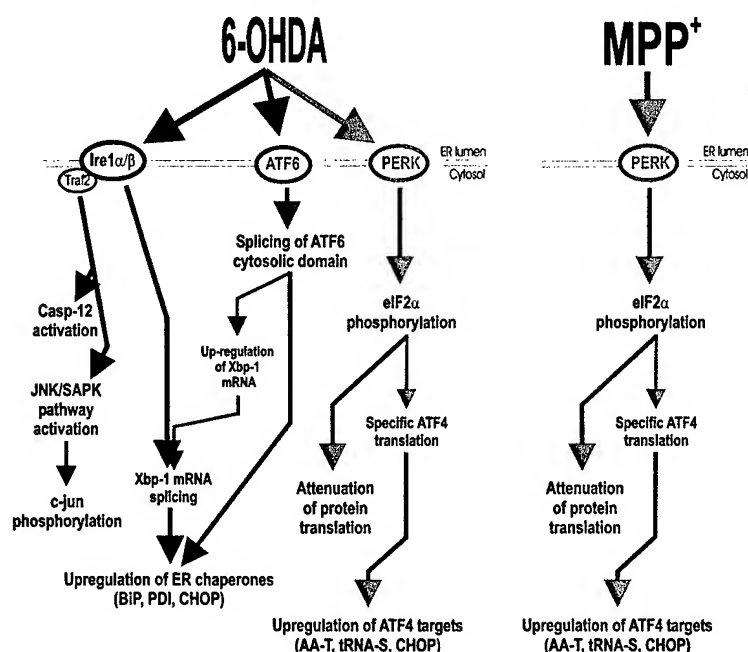


Fig. 1. 6-OHDA induces multiple targets of UPR, while MPP⁺ is restricted to the PERK pathway. The mammalian UPR consists of three ER membrane resident proteins (Ire1 α/β , ATF6, and PERK) that sense ER stress and activate the UPR pathway resulting in transcriptional changes and attenuation of protein translation. The current studies demonstrate that 6-OHDA induces all three arms of the UPR leading ultimately to the transcriptional changes first identified by microarray analysis. In contrast, MPP⁺ is restricted to phosphorylation of PERK and eIF2 α , resulting in up-regulation of a subset of genes induced by 6-OHDA (Holtz and O'Malley, 2003).

To aid in analyzing additional transcriptional changes generated from the 9-hour time point and our anticipated new data from the one and 6-hour points, we have developed protocols to analyze transcript levels using real time PCR. As an example, new primers for CHOP cDNA were prepared and used to reverse-transcribe total RNA from MN9D cells exposed to 6-OHDA or MPP⁺ for 0, 1, 3, 6, 9, or 12 hours. This cDNA was then analyzed using real time PCR. cDNA from the constitutively transcribed GAPDH gene was also analyzed to normalize the

CHOP values. The resulting data were used to determine the relative-fold induction of CHOP as a function of time exposed to 6-OHDA or MPP⁺. As shown in Fig. 2, the real time PCR results verified previous data indicating that CHOP is induced up to 6 and 8 fold by MPP⁺ and 6-OHDA, respectively.

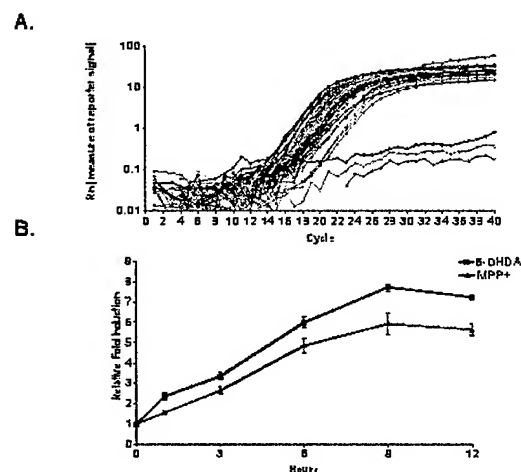


Fig. 2. Real time PCR confirms microarray results: CHOP is upregulated by MPP⁺ and 6-OHDA.

eIF2 α and c-jun. In contrast, none of the markers seen in the dopaminergic cell line were up regulated in mesencephalic cultures treated with MPP⁺.

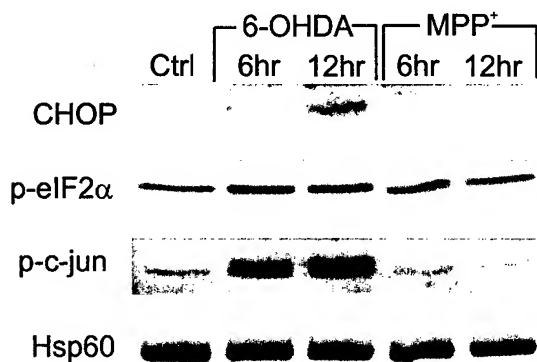


Fig. 3. 6-OHDA up-regulates CHOP in primary mesencephalic neurons. Protein lysates were prepared from primary mesencephalic cultures treated with 6-OHDA and MPP⁺. Western blot analysis of primary lysates was done using antibodies against CHOP, phosphorylated eIF2 α (p-eIF2 α), phosphorylated c-jun (p-c-jun), and Hsp60 as a protein loading control.

D. Are neurotoxin-mediated changes in gene expression recapitulated in cultured dopaminergic neurons?

To confirm and extend results obtained using the dopaminergic cell line model, we are using primary cultures of dopaminergic neurons. The advantages of using this paradigm include the ease of preparation and culture manipulation and the well-documented similarity in responses (Oh et al., 1995; Lotharius et al., 1999; Holtz and O'Malley, 2003). To determine whether UPR induction could be observed in mesencephalic cultures following neurotoxin treatment, Western blot analysis and immunocytochemistry were performed. Similar to results from the dopaminergic MN9D cells, 6-OHDA increased levels of CHOP protein at 6 and 12 hours (Fig. 3). 6-OHDA also increased phosphorylation of

Immunostaining of primary cultures with CHOP and phospho-c-jun antibodies allowed individual dopaminergic neurons to be examined via co-staining with TH. 6-OHDA treated cultures displayed intense nuclear staining of CHOP in both dopaminergic neurons as well as in many other cell types (Fig. 4). Cultures treated with MPP⁺ did not appear different from controls in overall expression of CHOP, nor was CHOP induction detected in dopaminergic neurons over a 24-hour period. Similarly, increased expression of phospho-c-jun was widespread with 6-OHDA treatment in both dopaminergic and non-dopaminergic neurons, whereas there was no obvious change in phosphorylation of c-jun following MPP⁺ administration. Taken together, these results suggest that MPP⁺ can induce a partial UPR response in the MN9D cell line but not in cultured dopaminergic neurons. In contrast, 6-OHDA induces a broad spectrum of UPR

responses in both MN9D cells as well as in dissociated dopaminergic neurons. Thus, these cells will serve as a useful model in determining the temporal and molecular events associated with 6-OHDA neurotoxicity. As new data become available from our additional microarray

experiments, we will continue screening both the MN9D cells as well as our primary culture model to confirm and extend these results.

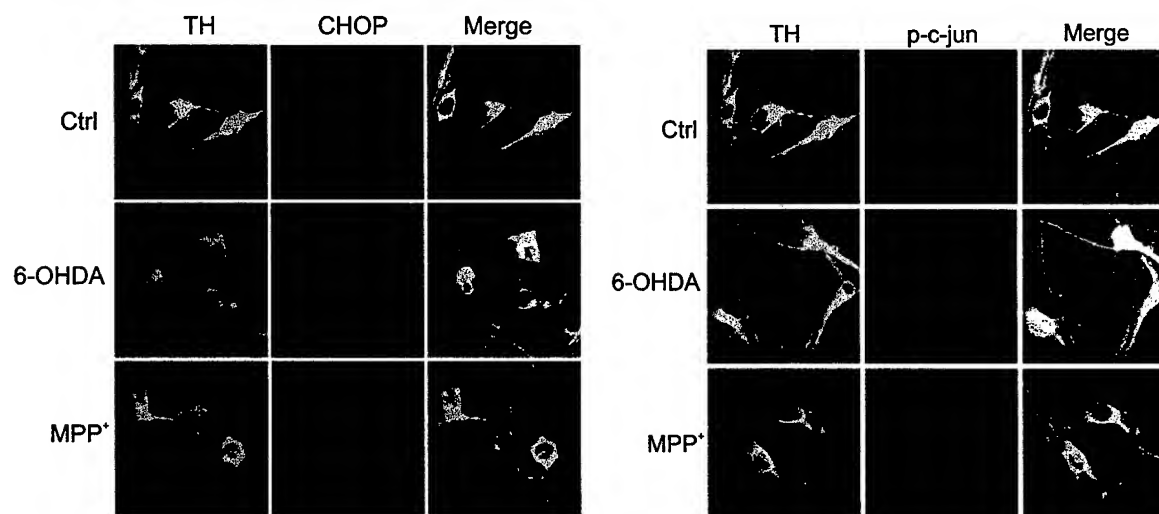


Fig. 4. 6-OHDA up-regulates CHOP and p-c-jun in dissociated dopaminergic neurons. Primary cultures treated for 18 hours were fixed and stained for CHOP and TH. Primary cultures treated for 12 hours were fixed and stained for phospho-c-jun and TH.

What are the signaling pathways involved in this response? In contrast to the well-delineated mitochondrial-mediated cell death pathways, ER stress/UPR signaling cascades are still unclear. Because identification of the initiators of this process will allow new therapeutic avenues to be pursued, we have used our microarray data to identify molecules that might be involved in this response. Potential candidates include the cysteinyl aspartate proteinases (caspases) that mediate programmed cell death and/or the so-called BH3-only proteins that affect many cellular processes to trigger cell death responses.

Inasmuch as caspase 12 specifically localizes to ER membranes and has been shown to be cleaved in the course of ER stress/UPR mediated cell death (Nakagawa et al., 2000), caspase 12 is a prime candidate for being the "ER stress mediator". To test this hypothesis we looked for evidence of caspase 12 involvement in our model. Surprisingly, antibodies that easily recognized caspase 12 activation in control cells were unable to detect similarly sized proteins in either our dopaminergic cell line or primary culture model. Moreover, our microarray results suggested that caspase 12 transcripts were not present nor could we directly amplify caspase 12 fragments using RT/PCR. Finally pre-treatment with inhibitors of the caspase 12 activators, calpains (I, II) failed to prevent CHOP or caspase 3 activation. Therefore, it would not appear that caspase 12 is triggering neurotoxin-mediated dopaminergic cell death.

As indicated in Table 6, only caspase 2,3,7, and 9 are expressed in the MN9D cells. Because very recent studies have shown that caspase 2 may serve as an initiating caspase particularly in models that also involve ER stress/UPR (e.g. β -amyloid toxicity; Troy and Shelanski, 2003), we screened our dopaminergic model for the presence and activation of caspase 2. Briefly, no evidence of caspase 2 activation was observed using real-time PCR, Western blotting techniques, activity assays, and/or caspase 2 inhibitors. Thus it would appear that caspase 2 does not initiate cell death in this system. Previously we've shown caspase 3 activation beginning around 6 hours after 6-OHDA treatment (Jensen et al., 2003). Caspase 7 and 9 are also activated within that time frame (not shown).

The results described above have re-focused our attention on the BH3-only proteins. Previously, we have determined that pro-apoptotic Bax is not involved since Bax deficient animals do not rescue primary dopaminergic neurons from 6-OHDA or MPP⁺-mediated cell death (O'Malley et al., 2003). Similarly we've ruled out Bad and Bak (not published). However, this is a large family of proteins and new ones are discovered with regularity. We are in the process of systematically testing every known BH3-only protein as a possible mediator of this response. For example, BH3-only proteins, Bim and Bid are present in MN9D cells although their transcript levels do not change following 6-OHDA or MPP⁺ treatment (Table 6), nor do their protein levels (not shown). Another BH3-only protein recently shown to mediate ER stress/UPR cell death is Bbc3/PUMA (Reimertz et al., 2003). Because this gene is not on the microarray that we originally screened, we're using PCR based methodologies to determine whether it is present in MN9D cells and/or primary mesencephalic cultures and whether it is induced in response to ER stress/UPR.

Key Research Accomplishments

Analyzed hybridization patterns of normal and 9-hour toxin-treated cRNAs using in-house GeneChip Facility and Affymetrix 12,000 gene chip set.

Verified differential regulation of particular gene subsets using RNA, Western blot, and immunocytochemical analysis in MN9D cells and cultured dopaminergic neurons.

Discovered that both MPP⁺ and 6-OHDA induce markers of ER stress.

Prepared mRNA from normal, 6-OHDA and MPP⁺-treated dopaminergic cells at 1 and 6 hours post treatment.

Established real time PCR techniques to evaluate microarray data.

Initiated delineation of signaling pathways mediating neurotoxin responses.

Reportable Outcomes

A poster describing our initial studies was presented at the Society for Neuroscience Annual Meeting, 2002.

A slide presentation describing our current studies will be presented at the Society for Neuroscience Annual Meeting, 2003.

Initial studies were published as: Holtz WA and O'Malley KL (2003) Parkinsonian mimetics induce aspects of unfolded protein response in death of dopaminergic neurons. J Biol Chem. 278:19367-77. Epub 2003 Feb 21.

Conclusions

The central hypothesis of these studies is that changes in gene expression underlie much of the damage that ultimately leads to the death of dopaminergic neurons after treatment with 6-OHDA

or MPP⁺. Using DNA microarray technology we determined that both of these neurotoxins induce ER stress although not to the same degree. Identification of key genetic components of this response may suggest new points of intervention. Taken together, these experiments will help clarify the molecular mechanisms associated with 6-OHDA and MPP⁺ toxicity and might aid in developing novel therapeutic avenues to pursue relevant to PD.

References

- Betarbet R, Sherer TB, Di Monte DA, Greenamyre JT. (2002) Mechanistic approaches to Parkinson's disease pathogenesis. *Brain Pathol.* 12:499-510.
- Choi WS, Yoon SY, Oh TH, Choi EJ, O'Malley KL, Oh YJ. Two distinct mechanisms are involved in 6-hydroxydopamine- and MPP⁺-induced dopaminergic neuronal cell death: role of caspases, ROS, and JNK. *J Neurosci Res.* 1999 57:86-94.
- Holtz WA, O'Malley KL. (2003) Parkinsonian mimetics induce aspects of unfolded protein response in death of dopaminergic neurons. *J Biol Chem.* 278:19367-77.
- Imai Y, Soda M, Inoue H, Hattori N, Mizuno Y, Takahashi R. (2001) An unfolded putative transmembrane polypeptide, which can lead to endoplasmic reticulum stress, is a substrate of Parkin. *Cell.* 105:891-902.
- Jensen PJ, Alter BJ, O'Malley KL. (2003) Alpha-synuclein protects naive but not dbcAMP-treated dopaminergic cell types from 1-methyl-4-phenylpyridinium toxicity. *J Neurochem.* 86:196-209.
- Kitada T, Asakawa S, Hattori N, Matsumine H, Yamamura Y, Minoshima S, Yokochi M, Mizuno Y, and Shimizu N (1998): Mutations in the parkin gene cause autosomal recessive juvenile parkinsonism. *Nature* 392:605-8.
- Kruger R, Kuhn W, Muller T, Woitalla D, Graeber M, Kosel S, Przuntek H, Epplen JT, Schols L, and Riess O (1998): Ala30Pro mutation in the gene encoding alpha-synuclein in Parkinson's disease. *Nat Genet* 18:106-8.
- Lotharius J., Dugan L.L., O'Malley K.L. (1999) Distinct mechanisms underlie neurotoxin-induced cell death in cultured dopaminergic neurons. *J. Neurosci.* 19: 1284-1293.
- McNaught KS, Mytilineou C, Jnobaptiste R, Yabut J, Shashidharan P, Jennert P, Olanow CW. (2002a) Impairment of the ubiquitin-proteasome system causes dopaminergic cell death and inclusion body formation in ventral mesencephalic cultures. *J Neurochem.* 81:301-6.
- McNaught KS, Bjorklund LM, Belizaire R, Isacson O, Jenner P, Olanow CW. (2002b) Proteasome inhibition causes nigral degeneration with inclusion bodies in rats. *Neuroreport.* 13:1437-41.
- Nakagawa T, Zhu H, Morishima N, Li E, Xu J, Yankner BA, Yuan J. (2000) Caspase-12 mediates endoplasmic-reticulum-specific apoptosis and cytotoxicity by amyloid-beta. *Nature.* 403:98-103.

Oh Y.J., Wong S.C., Moffat M., O'Malley K.L. (1995) Overexpression of Bcl-2 attenuates MPP+, but not 6-OHDA-induced cell death in a dopaminergic neuronal cell line. *Neurobiol. Dis.* 2: 157-167.

O'Malley KL, Liu J, Lotharius J, Holtz W. (2003) Targeted expression of BCL-2 attenuates MPP(+) but not 6-OHDA induced cell death in dopaminergic neurons. *Neurobiol Dis.* 14:43-51.

Reimertz C, Kogel D, Rami A, Chittenden T, Prehn JH. (2003) Gene expression during ER stress-induced apoptosis in neurons: induction of the BH3-only protein Bbc3/PUMA and activation of the mitochondrial apoptosis pathway. *J Cell Biol.* 162:587-97.

Ryu EJ, Harding HP, Angelastro JM, Vitolo OV, Ron D, Greene LA. (2002) Endoplasmic reticulum stress and the unfolded protein response in cellular models of Parkinson's disease. *J Neurosci.* 22:10690-8.

Shimura H, Hattori N, Kubo S, Mizuno Y, Asakawa S, Minoshima S, Shimizu N, Iwai K, Chiba T, Tanaka K, Suzuki T. (2000) Familial Parkinson disease gene product, parkin, is a ubiquitin-protein ligase. *Nat Genet.* 25:302-5.

Spillantini MG, Schmidt ML, Lee VM, Trojanowski JQ, Jakes R, Goedert M. (1997) Alpha-synuclein in Lewy bodies. *Nature.* 388:839-40.

Troy CM, Shelanski ML. (2003) Caspase-2 redux. *Cell Death Differ.* 10:101-7.

Tsai YC, Fishman PS, Thakor NV, Oyler GA. (2003) Parkin facilitates the elimination of expanded polyglutamine proteins and leads to preservation of proteasome function. *J Biol Chem.* 278:22044-55.

Table 1. Transcripts increased by MPP*.

GenBankID	GeneSymbol	GeneName	fold change		Signal log ratio	
			MPP*	6-OHDA	MPP*	6-OHDA
X67083	Ddit3	DNA-damage inducible transcript 3	9.2	26.0	3.2	4.7
AA770736	Ifid2	induced in fatty liver dystrophy 2	4.4	4.0	2.2	4.0
M61007	Cebpb	CCAAT/enhancer binding protein C/EBP beta	4.0	4.6	2.0	2.2
A1852641	P8-pending	p8 protein	3.9	5.3	2.0	2.4
AW124369	Gtpbp2	GTP binding protein 2	3.2	2.9	1.7	1.6
A1849556		ESTs	3.1	2.3	1.7	1.2
A1839690	1500005G05Rik	RIKEN cDNA 1500005G05 gene	3.1	3.9	1.7	2.0
U19118	Atf3	activating transcription factor 3	2.6	9.8	1.4	3.3
A1849939	5830413E08Rik	RIKEN cDNA 5830413E08 gene	2.5	1.7	1.4	0.8
A1854851		ESTs	2.5	1.1	1.3	0.2
U75215	Sic1a4	neutral amino acid transporter	2.4	1.7	1.3	0.8
X51829	Myd116	myeloid differentiation primary response gene 116	2.3	4.3	1.2	2.1
A1848732	Cars	cysteinyl-tRNA synthetase	2.1	2.2	1.1	1.2
X95761	Lbcd1	lymphoid blast crisis-like 1	2.1	2.5	1.1	1.4
A1838015	1200017E13Rik	RIKEN cDNA 1200017E13 gene	2.1	2.8	1.1	1.5
A1846545		Mus musculus Similar to phosphoserine phosphatase clone MGC 7574 mRNA complete cds	2.0	1.7	1.0	0.8
U28656	Elf4ebp1	eukaryotic translation initiation factor 4E binding protein 1	2.0	1.6	1.0	0.7
U63387	Cbx4	chromobox homolog 4 Drosophila Pc class	2.0	1.3	1.0	0.4
M94087	Atf4	activating transcription factor 4	1.9	2.0	1.0	1.0
AB017189	Sic7a5	solute carrier family 7 cationic amino acid transporter y system member 5	1.9	1.5	1.0	0.6
X78709	Nfe211	nuclear factor erythroid derived 2 like 1	1.9	1.6	1.0	0.7
U40930	Sqstm1	sequestosome 1	1.9	7.0	0.9	2.8
A1845237	Clic4	chloride intracellular channel 4 mitochondrial	1.8	1.5	0.9	0.6
AW122372	D10Bwg0791e	DNA segment Chr 10 Brigham Women s Genetics 0791 expressed	1.8	0.5	0.9	-1.2
A1849533	Clic4	chloride intracellular channel 4 mitochondrial	1.7	1.5	0.8	0.6
AA684508		ESTs	1.7	4.0	0.8	2.0
A1849620		Mus musculus 10 days embryo cDNA RIKEN full-length enriched library clone 2600002G09	1.7	1.9	0.8	1.0
AW125480	Gas5	ESTs Weakly similar to 16.7Kd protein [H.sapiens]	1.7	1.4	0.8	0.5
A1849615		growth arrest specific 5	1.7	2.1	0.8	1.1
A1854884	2610007K22Rik	RIKEN cDNA 2610007K22 gene	1.7	0.8	0.8	-0.4
A1844089		ESTs Highly similar to LEUCYL-TRNA SYNTHETASE CYTOPLASMIC [Saccharomyces cerevisiae]	1.7	1.8	0.8	0.9
X67056	Glyt1	glycine transporter 1	1.7	1.6	0.8	0.7
A1839392		ESTs Highly similar to ALANYL-TRNA SYNTHETASE [Homo sapiens]	1.7	1.9	0.8	0.9
AF023482	Hax1-pending	HS1 binding protein	1.7	1.8	0.8	0.9
A1839918		Mus musculus 10 11 days embryo cDNA RIKEN full-length enriched library clone 2810017N01	1.6	1.5	0.7	0.6
X54327		M. musculus mRNA for glutamyl-tRNA synthetase	1.6	1.5	0.7	0.6
A1836408		ESTs Weakly similar to CG11414 gene product [D.melanogaster]	1.6	1.4	0.7	0.5
X76505	Ddr2	discoidin domain receptor family member 2	1.6	1.6	0.7	0.7
X14309	Mdu1	antigen identified by monoclonal antibodies 4F2	1.6	2.2	0.7	1.2
AW125874	3010001M15Rik	RIKEN cDNA 3010001M15 gene	1.6	1.7	0.7	0.8
A1852087	1200017E04Rik	RIKEN cDNA 1200017E04 gene	1.6	0.8	0.7	-0.3
A1851163	Wars	tryptophanyl-tRNA synthetase	1.6	1.6	0.7	0.7
J04627	Mthfd2	methylenetetrahydrofolate dehydrogenase NAD dependent methenyltetrahydrofolate cyclohydrolase	1.6	1.3	0.7	0.4
D17666		Mus musculus clone IMAGE 3491909 mRNA partial cds	1.5	1.6	0.6	0.7
A1848393		RIKEN cDNA 1200003J13 gene	1.5	1.4	0.6	0.5
AW060270	1200003J13Rik		1.5	1.1	0.6	0.2

Table 1. Transcripts increased by MPP⁺.

GenBankID	GeneSymbol	GeneName	fold change		Signal log ratio	
			MPP ⁺	6-OHDA	MPP ⁺	6-OHDA
AA798624	Ero1l-pending	ERO1-like <i>S. cerevisiae</i>	1.5	1.5	0.6	0.6
AI929971	1010001P14Rik	RIKEN cDNA 1010001P14 gene	1.5	1.7	0.6	0.8
AI841996	D12Bwg0579e	DNA segment Chr 12 Brigham Women s Genetics 0579 expressed	1.5	1.3	0.6	0.4
AF004294	Myt1	myelin transcription factor 1	1.5	1.2	0.6	0.3
AI845237	Clic4	chloride intracellular channel 4 mitochondrial	1.5	1.2	0.6	0.3
AW120614	Ero1l-pending	ERO1-like <i>S. cerevisiae</i>	1.5	1.7	0.6	0.8
AI849432	Clcn3	chloride channel 3	1.5	1.8	0.6	0.9
AF103809	Ap3b1	adaptor-related protein complex AP-3 beta 1 subunit	1.5	1.2	0.6	0.3
AI853918		ESTs Weakly similar to PRP3 MOUSE PROLINE-RICH PROTEIN MP-3 [M.musculus]	1.5	0.8	0.6	-0.3

Table 2. Transcripts decreased by MPP⁺.

GenBankID	GeneSymbol	GeneName	fold change		Signal log ratio	
			MPP ⁺	6-OHDA	MPP ⁺	6-OHDA
AJ002387	Hspa5	heat shock 70kD protein 5 glucose-regulated protein 78kD	0.5	3.0	-1.2	1.6
AW106745	Nsdh1	NAD P dependent steroid dehydrogenase-like	0.5	0.5	-1.1	-1.0
M14223	Rrm2	ribonucleotide reductase M2	0.5	0.5	-1.1	-1.2
X13135	Fasn	fatty acid synthase	0.5	0.5	-1.0	-1.0
X54401			0.6	1.2	-0.8	0.3
Z19521	Ldlr	low density lipoprotein receptor	0.6	0.6	-0.8	-0.8
D42048	Sqle	squalene epoxidase	0.6	0.6	-0.7	-0.7
M21285			0.6	0.5	-0.7	-0.9
AF020185	Dncl1	dynein cytoplasmic light chain 1	0.7	1.0	-0.6	-0.1
A1848479		ESTs Weakly similar to open reading frame [M.musculus]	0.7	0.6	-0.6	-0.8
AW045533		ESTs Highly similar to FARNESYL PYROPHOSPHATE SYNTHETASE	0.7	0.9	-0.6	-0.1
X62154	Mcmd	mini chromosome maintenance deficient S. cerevisiae	0.7	0.7	-0.6	-0.5
AW227650	0610038P07Rik	RIKEN cDNA 0610038P07 gene	0.7	1.3	-0.6	0.4
A1846851		ESTs Highly similar to FARNESYL PYROPHOSPHATE SYNTHETASE	0.7	1.0	-0.6	0.1
AA529583	Mrgx-pending	MORF-related gene X	0.7	1.2	-0.5	0.3

Table 3. Transcripts increased by both 6-OHDA and MPP⁺.

GenBankID	GeneSymbol	GeneName	fold change		Signal log ratio	
			6-OHDA	MPP ⁺	6-OHDA	MPP ⁺
X67083	Ddit3	DNA-damage inducible transcript 3	26.0	9.2	4.7	3.2
U19118	Aif3	activating transcription factor 3	9.8	2.6	3.3	1.4
U40930	Sqstm1	sequestosome 1	7.0	1.9	2.8	0.9
AI952641	P8-pending	p8 protein	5.3	3.9	2.4	2.0
M61007	Cebpb	CCAAT/enhancer binding protein C/EBP beta	4.6	4.0	2.2	2.0
X51829	Myd116	myeloid differentiation primary response gene 116	4.3	2.3	2.1	1.2
AA684508		ESTs	4.0	1.7	2.0	0.8
AA770736	Ifid2	induced in fatty liver dystrophy 2	4.0	4.4	2.0	2.2
AI839690	1500005G05Rik	RIKEN cDNA 1500005G05 gene	3.9	3.1	2.0	1.7
AW124369	Gtpbp2	GTP binding protein 2	2.9	3.2	1.6	1.7
AI838015	1200017E13Rik	RIKEN cDNA 1200017E13 gene	2.8	2.1	1.5	1.1
X95761	Lbcl1	lymphoid blast crisis-like 1	2.5	2.1	1.4	1.1
X14309	Mdu1	antigen identified by monoclonal antibodies 4F2	2.2	1.6	1.2	0.7
AI848732	Cars	cysteiny/1-RNA synthetase	2.2	2.1	1.2	1.1
AI849615	Gas5	growth arrest specific 5	2.1	1.7	1.1	0.8
M94087	Aif4	activating transcription factor 4	2.0	1.9	1.0	1.0
AI839392		ESTs Highly similar to ALANYL-TRNA SYNTHETASE [Homo sapiens]	1.9	1.7	1.0	0.8
AF023482	Hax1-pending	Mus musculus 10 days embryo cDNA RIKEN full-length enriched library clone 2600002G09	1.9	1.7	0.9	0.8
AI849432	Cicn3	HS1 binding protein	1.8	1.7	0.9	0.8
AI844089		chloride channel 3	1.8	1.5	0.9	0.6
AI846545		ESTs Highly similar to LEUCYL-TRNA SYNTHETASE CYTOPLASMIC [Saccharomyces cerevisiae]	1.8	1.7	0.9	0.8
AW125874	3010001M15Rik	Mus musculus Similar to phosphoserine phosphatase clone MGC 7574 mRNA complete cds	1.7	2.0	0.8	1.0
U75215	Slc1a4	RIKEN cDNA 3010001M15 gene	1.7	1.6	0.8	0.7
AW120614	Ero1l-pending	neutral amino acid transporter	1.7	2.4	0.8	1.3
AI929971	1010001P14Rik	ERO1-like S. cerevisiae	1.7	1.5	0.8	0.6
AI849939	5830413E08Rik	RIKEN cDNA 1010001P14 gene	1.7	1.5	0.8	0.6
AI851163	Wars	RIKEN cDNA 5830413E08 gene	1.7	2.5	0.8	1.4
U28656	Elf4ebp1	tryptophanyl-tRNA synthetase	1.6	1.6	0.7	0.7
X67056	Glyt1	eukaryotic translation initiation factor 4E binding protein 1	1.6	2.0	0.7	1.0
X76505	Ddr2	glycine transporter 1	1.6	1.7	0.7	0.8
D17666		discoidin domain receptor family member 2	1.6	1.6	0.7	0.7
X78709	Nfe2l1	nuclear factor erythroid derived 2 like 1	1.6	1.5	0.7	0.6
AI849533	Clic4	chloride intracellular channel 4 mitochondrial	1.5	1.7	0.6	0.8
X54327		M. musculus mRNA for glutamyl-tRNA synthetase	1.5	1.6	0.6	0.7
AA798624	Ero1l-pending	ERO1-like S. cerevisiae	1.5	1.5	0.6	0.6
AI839918		Mus musculus 10 11 days embryo cDNA RIKEN full-length enriched library clone 2810017N01	1.5	1.6	0.6	0.7
AI845237	Clic4	chloride intracellular channel 4 mitochondrial	1.5	1.8	0.6	0.9
AB017189	Slc7a5	solute carrier family 7 cationic amino acid transporter y system member 5	1.5	1.9	0.6	1.0

Table 4. Transcripts increased by 6-OHDA

GenBankID	GeneSymbol	GeneName	fold change		Signal log ratio	
			6-OHDA	MPP*	6-OHDA	MPP*
X67083	Ddit3	DNA-damage inducible transcript 3	26.0	9.2	4.7	3.2
U19118	Atf3	activating transcription factor 3	9.8	2.6	3.3	1.4
AW120711	DnaJb9	DNA J protein b9	7.0	0.7	2.8	-0.6
U40930	Sqstm1	sequestosome 1	7.0	1.9	2.8	0.9
AI846938	Herpud1	homocysteine-inducible endoplasmic reticulum stress-inducible ubiquitin-like domain member 1	6.5	1.3	2.7	0.4
AF105222	Lag1-pending	leukemia-associated gene-like	6.1	1.3	2.6	0.4
X56824	Hmox1	heme oxygenase decycling 1	5.7	1.5	2.5	0.6
AI852641	P8-pending	p8 protein	5.3	3.9	2.4	2.0
M61007	Cebpb	CCAAT/enhancer binding protein C/EBP beta	4.6	4.0	2.2	2.0
AJ011967	Gdf15	growth differentiation factor 15	4.4	3.0	2.2	1.6
X51829	Myd116	myeloid differentiation primary response gene 116	4.3	2.3	2.1	1.2
AA684508		ESTs	4.0	1.7	2.0	0.8
AA770736	Ildl2	induced in fatty liver dystrophy 2	4.0	4.4	2.0	2.2
AI839690	1500005G05Rik	RIKEN cDNA 1500005G05 gene	3.9	3.1	2.0	1.7
AW123904	3110025G09Rik	RIKEN cDNA 3110025G09 gene	3.7	1.2	1.9	0.3
AI845538	Etv6	ets variant gene 6 TEL oncogene	3.6	0.6	1.9	-0.8
AW121716	0610031F24Rik	RIKEN cDNA 0610031F24 gene	3.0	1.0	1.6	-0.1
AW122364	3230402M22Rik	RIKEN cDNA 3230402M22 gene	3.0	0.4	1.6	-1.5
AJ002387	Hspa5	heat shock 70kD protein 5 glucose-regulated protein 78kD	3.0	0.5	1.6	-1.2
AW124369	Gbbp2	GTP binding protein 2	2.9	3.2	1.6	1.7
X61940	Ptpn16	protein tyrosine phosphatase non-receptor type 16	2.9	1.1	1.6	0.2
X67644	Ier3	immediate early response 3	2.8	1.1	1.5	0.2
AI838015	1200017E13Rik	RIKEN cDNA 1200017E13 gene	2.8	2.1	1.5	1.1
AV305832	Ubc	ubiquitin C	2.8	0.8	1.5	-0.3
AW122851	1110002O23Rik	RIKEN cDNA 1110002O23 gene	2.7	0.7	1.5	-0.5
AI843420	Bag3	Bcl2-associated athanogene 3	2.6	1.0	1.4	-0.1
AW045202	1700015E05Rik	RIKEN cDNA 1700015E05 gene	2.5	0.5	1.4	-0.9
AI839280	1810045K07Rik	RIKEN cDNA 1810045K07 gene	2.5	1.4	1.4	0.5
X95761	Lbcl1	lymphoid blast crisis-like 1	2.5	2.1	1.4	1.1
U95053	Gclm	glutamate-cysteine ligase modifier subunit	2.5	1.0	1.4	-0.1
J03297	Tra1	tumor rejection antigen gp96	2.3	0.8	1.2	-0.4
AW045202	1700015E05Rik	RIKEN cDNA 1700015E05 gene	2.3	0.5	1.2	-1.0
AW122690		ESTs	2.3	0.7	1.2	-0.5
X14309	Mdu1	antigen identified by monoclonal antibodies 4F2	2.2	1.6	1.2	0.7
AI848732	Cars	cysteinyI-tRNA synthetase	2.2	2.1	1.2	1.1
AI837625	Csrp	cysteine rich protein	2.2	1.1	1.2	0.2
D88793	Csrp	cysteine rich protein	2.1	1.0	1.1	0.0
AI848343	Sec23b	SEC23B S. cerevisiae	2.1	1.0	1.1	0.0
AI849615	Gas5	growth arrest specific 5	2.1	1.7	1.1	0.8
AI845293	1500032E05Rik	RIKEN cDNA 1500032E05 gene	2.1	1.0	1.1	-0.1
AF100956	Sacm2l	SAC2 supressor of actin mutations 2 homolog like S. cerevisiae	2.1	1.0	1.1	0.1
D17571	Por	P450 cytochrome oxidoreductase	2.1	1.0	1.1	0.1
AW122075	251000110Rik	RIKEN cDNA 251000110 gene	2.1	0.9	1.1	-0.1
AI837395		ESTs Highly similar to SERYL-TRNA SYNTHETASE [Cricetulus griseus]	2.0	1.4	1.0	0.5
M94087	Atf4	activating transcription factor 4	2.0	1.9	1.0	1.0
D50527	Ubc	ubiquitin C	2.0	1.0	1.0	-0.1

Table 4. Transcripts increased by 6-OHDA

GenBankID	GeneSymbol	GeneName	fold change	Signal log ratio
D49733		Mus musculus 10 days embryo cDNA RIKEN full-length enriched library clone 2600002G09 full insert sequence	1.9	1.0
A1849620		tryptophanyl-tRNA synthetase	1.9	1.0
X69656	Wars	RIKEN cDNA 2600001N01 gene	1.9	1.0
AW060179	2600001N01Rik	thioredoxin reductase 1	1.9	0.8
AB027565	Txnd1	RIKEN cDNA 3110001N18 gene	1.9	0.1
AW121568	3110001N18Rik	ESTs Highly similar to ALANYL-TRNA SYNTHETASE [Homo sapiens]	1.9	0.5
A1839392		avian reticuloendotheliosis viral v-rel oncogene homolog A	1.9	0.8
M61909	Rela	RIKEN cDNA 4922501H04 gene	1.9	0.2
A1836718	4922501H04Rik	signal peptidase complex 18kD	1.9	0.9
AB025405	Spc18-pending	solute carrier family 35 UDP-galactose transporter member 2	1.9	0.0
D87990	Slc35a2	ESTs	1.9	0.1
A1157060		RIKEN cDNA 2600001N01 gene	1.9	0.9
AW123786	2600001N01Rik	metallothionein 1	1.8	0.7
V00835	Mt1	RIKEN cDNA 2400002C15 gene	1.8	0.2
A1846849	2400002C15Rik	HS1 binding protein	1.8	0.9
AF023482	Hax1-pending	guanine nucleotide binding protein G protein gamma 3 subunit	1.8	0.8
AF069953	Gng3	RIKEN cDNA 1300009F09 gene	1.8	0.0
A1851062	1300009F09Rik	p10n protein	1.8	0.7
M18070	Pmp	aplysia ras-related homolog B RhoB	1.8	0.5
X99963	Arhb	chloride channel 3	1.8	0.9
A1849432	Clcn3	ESTs Highly similar to LEUCYL-TRNA SYNTHETASE CYTOPLASMIC [Saccharomyces cerevisiae]	1.8	0.6
A1844089		Mus musculus Similar to phosphoserine phosphatase clone MGC 7574 mRNA complete cds	1.7	0.8
A1846545		RIKEN cDNA 2310032N09 gene	1.7	0.2
A1847904	2310032N09Rik	Mus musculus 10 day old male pancreas cDNA RIKEN full-length enriched library clone 1810031C14	1.7	0.8
A1843732		RIKEN cDNA 061001012 gene	1.7	0.5
A1848699	061001012Rik	RIKEN cDNA 2410015H04 gene	1.7	0.8
A1841377	2410015H04Rik	RIKEN cDNA 3010001M15 gene	1.7	0.1
AW125874	3010001M15Rik	EST X83328	1.7	0.7
AW211667	X83328	Mus musculus mRNA for erythroid differentiation regulator partial	1.7	0.5
AJ007909		procollagen-proline 2-oxoglutarate 4-dioxygenase proline 4-hydroxylase alpha II polypeptide	1.7	0.8
U16163	P4ha2	neutral amino acid transporter	1.7	0.5
U75215	Slc1a4	X-linked lymphocyte-regulated 3b	1.7	1.3
L22977	Xlr3b	ESTs Moderately similar to hypothetical protein [H.sapiens]	1.7	0.8
A1159572		Mus musculus adult male liver cDNA RIKEN full-length enriched library clone 1300018P04 full insert sequence	1.7	0.2
A1848798		RIKEN cDNA 2310008M10 gene	1.7	0.8
A1848235	D6Vsu137e	DNA segment Chr 6 Wayne State University 137 expressed	1.7	-0.2
A1846708	Xbp1	ERO1-like S. cerevisiae	1.7	-0.3
AW123880	Ero1-pending	heat shock protein cognate 70 testis	1.7	-0.6
AW120614	Hsc70i	RIKEN cDNA 1110020C13 gene	1.7	0.6
AF103905		RIKEN cDNA 1200003J11 gene	1.7	-0.1
A1846553	1200003J11Rik	transmembrane protein 4	1.7	0.3
A1843287	Tmem4	RIKEN cDNA 1010001P14 gene	1.7	0.2
AW125880	1010001P14Rik	membrane bound C2 domain containing protein	1.7	0.5
A1929971	Mbc2	RIKEN cDNA 5830413E08 gene	1.7	0.6
AF098633			1.7	0.2
A1849939			1.7	1.4

Table 4. Transcripts increased by 6-OHDA

GenBankID	GeneSymbol	GeneName	fold change	Signal log ratio
AA866971		ESTs Moderately similar to hypothetical protein [H.sapiens]	1.7	1.3
Y18505	D0HXS9928E	DNA segment human DXS9928E	1.7	1.2
Z84471	G6pd2	glucose-6-phosphate dehydrogenase 2	1.7	0.9
AF062071	Zfp216	zinc finger protein 216	1.7	1.0
AW121539	1110014C03Rik	RIKEN cDNA 1110014C03 gene	1.6	0.8
AW125736	1110003F06Rik	RIKEN cDNA 1110003F06 gene	1.6	0.8
AW047320	2600006O07Rik	RIKEN cDNA 2600006O07 gene	1.6	1.2
AI841920	D13Wsu115e	DNA segment Chr 13 Wayne State University 115 expressed	1.6	0.9
AJ010391		tryptophanyl-tRNA synthetase	1.6	1.1
AI851163	Wars	annexin A2	1.6	1.6
M14044	Anxa2	SEC23A S. cerevisiae	1.6	1.1
AI843665	Sec23a	glucose-6-phosphate dehydrogenase X-linked	1.6	1.0
Z11911	G6pdx	RIKEN cDNA 5930426111 gene	1.6	1.0
AW046691	5930426111Rik	RIKEN cDNA 3110079L04 gene	1.6	0.9
AA683712	3110079L04Rik	caseinolytic protease ATP-dependent E. coli proteolytic subunit homolog	1.6	1.1
AJ005253	Cipp	RIKEN cDNA 0610010112 gene	1.6	1.1
AI848699	0610010112Rik	eukaryotic translation initiation factor 4E binding protein 1	1.6	1.3
U28656	Eif4ebp1	glycine transporter 1	1.6	2.0
X67056	Glyt1	discoidin domain receptor family member 2	1.6	1.7
X76505	Ddr2	peptidylprolyl isomerase B	1.6	1.6
X58990	Ppib	ESTs Highly similar to arsenate resistance protein ARS2 [H.sapiens]	1.6	0.8
AI845953		ESTs	1.6	1.5
D17666		Mus musculus stress-associated endoplasmic reticulum protein 1 ribosome associated membrane protein 4	1.6	1.1
AI846118		RIKEN cDNA 5730406115 gene	1.6	0.8
AI843466	5730406115Rik	glucose regulated protein 58 kDa	1.6	0.7
AI839946	Gp58	metallothionein 2	1.6	1.0
M73329	Mt2	Jun proto-oncogene related gene d1	1.6	1.2
K02236		RIKEN cDNA 1810024J13 gene	1.6	1.3
J04509	Jund1	CD151 antigen	1.6	1.1
AI838735	1810024J13Rik	nuclear factor erythroid derived 2 like 1	1.6	1.9
AF033620	Cd151	chloride intracellular channel 4 mitochondrial	1.5	1.7
X78709	Nfe211	RIKEN cDNA 5730465C04 gene	1.5	1.0
AI849533	Clic4	proteasome prosome macropain 26S subunit non-ATPase 4	1.5	1.1
AI836446	Psm4	RIKEN cDNA 2610103L06 gene	1.5	1.1
AF013099	2610103L06Rik	eukaryotic translation initiation factor 3 subunit 8 110 kDa	1.5	1.4
AW125336	Eif3s8	M. musculus mRNA for glutamyl-tRNA synthetase	1.5	1.6
U67328		ERO1-like S. cerevisiae	1.5	1.5
X54327		cystatin B	1.5	1.1
AA798624	Ero1-pending	ESTs Highly similar to PRE-MRNA SPLICING FACTOR PRP6 [Saccharomyces cerevisiae]	1.5	1.1
U59807	Cstb	DNA segment Chr 7 Wayne State University 105 expressed	1.5	0.7
AW046847	D7Wsu105e	branched chain aminotransferase 1 cytosolic	1.5	1.4
AA388099	Bcat1	calcium binding protein A11 calgizarin	1.5	0.9
U42443	S100a10	SEC61 gamma subunit S. cerevisiae	1.5	0.9
M16465	Sec61g	suppressor of initiator codon mutations related sequence 1 S. cerevisiae	1.5	1.2
U11027			1.5	0.6
Z50159	Sui1-rs1		1.5	0.6

Table 4. Transcripts increased by 6-OHDA

GenBankID	GeneSymbol	GeneName	fold change		Signal log ratio	
			6-OHDA	MPP ⁺	6-OHDA	MPP ⁺
AF069954	Gng3lg	G protein gamma 3 linked gene	1.5	1.1	0.6	0.2
A1839918		Mus musculus 10 11 days embryo cDNA RIKEN full-length enriched library clone 2810017N01 full insert sequence	1.5	1.6	0.6	0.7
A1845237	Clic4	chloride intracellular channel 4 mitochondrial	1.5	1.8	0.6	0.9
AB025313	Uchl1	ubiquitin carboxy-terminal hydrolase L1	1.5	1.1	0.6	0.1
A1836034	1110003B01Rik	RIKEN cDNA 1110003B01 gene	1.5	1.0	0.6	0.1
AW122255		ESTs Moderately similar to T00076 hypothetical protein KIAA0462 [H.sapiens]	1.5	1.3	0.6	0.4
AW122052		Mus musculus mRNA for N-acetylneuraminic acid 9-phosphate synthetase complete cds	1.5	0.8	0.6	-0.4
A1153421		Mus musculus mRNA for erythroid differentiation regulator partial	1.5	1.1	0.6	0.2
X57349	Trfr	transferrin receptor	1.5	0.9	0.6	-0.1
AB017189	Slc7a5	solute carrier family 7 cationic amino acid transporter y system member 5	1.5	1.9	0.6	1.0
U11812	Ptpm	protein tyrosine phosphatase receptor-type N	1.5	1.1	0.6	0.2
L39879	Ftl1	ferritin light chain 1	1.5	1.1	0.6	0.2
X51703	Ubb	ubiquitin B	1.5	1.0	0.6	0.1
AU020229	Fzd3	frizzled homolog 3 Drosophila	1.5	0.9	0.6	-0.1
D87691	D6Erttd109e	DNA segment Chr 6 ERATO Doi 109 expressed	1.5	1.0	0.6	0.0

Table 5. Transcripts decreasing with 6-OHDA.

GenBankID	GeneSymbol	GeneName	fold change		Signal log ratio	
			6-OHDA	MPP*	6-OHDA	MPP*
M29260	Fasn	fatty acid synthase	0.2	1.0	-2.5	0.0
X13135	Trmpo	thymopoietin	0.5	0.5	-1.0	-1.0
AW046443	BI2-pending	immunosuperfamily protein BI2	0.5	1.0	-1.0	0.0
AF061260	Sox11	SRY-box containing gene 11	0.5	1.1	-1.0	0.1
AF009414	Cbfb	core binding factor beta	0.5	1.1	-1.0	0.1
D14572	1010001C05Rik	RIKEN cDNA 1010001C05 gene	0.5	0.9	-0.9	-0.2
M21285	Hmgb3	high mobility group box 3	0.5	0.7	-0.9	-0.5
AF022465	ESTs	Moderately similar to JC4928 histone H1x [H.sapiens]	0.5	0.6	-0.9	-0.7
AI851599	Ethoh6	ethanol induced 6	0.6	0.8	-0.9	-0.3
AI843895	Cbfb	core binding factor beta	0.6	0.9	-0.9	-0.2
L03279	Ccnb2	cyclin B2	0.6	1.2	-0.8	0.3
X66032	RIKEN cDNA 1810037117 gene	core binding factor beta	0.6	0.9	-0.8	-0.1
AW125347	RIKEN cDNA 1110038L14 gene	ESTs	0.6	1.1	-0.8	0.2
AA681998	mini chromosome maintenance deficient 2 S. cerevisiae	cyclin A2	0.6	0.8	-0.8	-0.3
AW120755	Cna2	GATA-binding protein 2	0.6	0.8	-0.8	-0.3
D86725	Gata2	squalene epoxidase	0.6	0.9	-0.8	-0.1
X75483	Sqle	septin 9	0.6	0.8	-0.7	-0.4
AB000096	9-Sep	neurofilament heavy polypeptide	0.6	0.8	-0.7	-0.1
D42048	Nfh	ESTs	0.6	0.8	-0.7	-0.2
AJ250723	Pcnt	pericentrin	0.6	0.8	-0.6	-0.4
M35131	Nek2	NIMA never in mitosis gene a related expressed kinase 2	0.7	0.9	-0.6	-0.1
AW047671	1810012N18Rik	RIKEN cDNA 1810012N18 gene	0.7	1.0	-0.6	-0.1
AI194767	Hmgb1	high mobility group box 1	0.7	0.8	-0.6	-0.4
AF013166	Mlp	MARCKS-like protein	0.7	0.8	-0.6	-0.4
AI839212	Bmi1	B lymphoma Mo-MLV insertion region 1	0.7	0.8	-0.6	-0.3
U00431	3110023F10Rik	RIKEN cDNA 3110023F10 gene	0.7	1.0	-0.6	0.0
X61399	Mcm4	mini chromosome maintenance deficient 4 homolog S. cerevisiae	0.7	0.9	-0.6	-0.2
M64068	Impnb	importin beta	0.7	1.3	-0.5	0.4
AI195392	Impnb	Mus musculus Pumilio 2 Pumm2 mRNA complete cds	0.7	0.7	-0.5	-0.6
X58196	Hnrpb	heterogeneous nuclear ribonucleoprotein A/B	0.7	1.0	-0.5	0.1
D26089	Cd24a	CD24a antigen	0.7	1.1	-0.5	0.1
D45836	ESTs	ESTs	0.7	0.9	-0.5	-0.2
AI837010			0.7	0.9	-0.5	-0.2
D90151			0.7	0.9	-0.5	-0.2
M58661			0.7	0.9	-0.5	-0.2
AI848984			0.7	1.0	-0.5	-0.1

Table 6. Transcripts Related to Programmed Cell Death

Gene	Control	MPP+	6-OHDA
caspase 1	absent	absent	absent
caspase 2	present	no change	no change
caspase 3	present	no change	no change
caspase 6	absent	absent	absent
caspase 7	present	no change	no change
caspase 8	absent	absent	absent
caspase 9	present	no change	no change
caspase 11/4	absent	absent	absent
caspase 12	absent	absent	absent
caspase 14	absent	absent	absent
apaf1	present	no change	no change
bax	present	no change	no change
bak	present	no change	no change
bad	present	no change	no change
boo/diva	absent	absent	absent
bim/bod	present	no change	no change
dp5/hrk	absent	absent	absent
bok	present	decreased	decreased
bid	present	no change	no change
bag1	present	no change	no change
bag2	present	no change	no change
bag3	present	no change	no change
bcl-2	absent	absent	absent
bcl-x	absent	absent	absent
bcl-w	absent	absent	absent
bcl-rambo	present	no change	no change

Parkinsonian Mimetics Induce Aspects of Unfolded Protein Response in Death of Dopaminergic Neurons*

Received for publication, November 20, 2002, and in revised form, February 19, 2003
Published, JBC Papers in Press, February 21, 2003, DOI 10.1074/jbc.M211821200

William Andrew Holtz and Karen Laurel O'Malley†

From the Anatomy and Neurobiology Department, Washington University School of Medicine, St. Louis, Missouri 63110

Genes associated with Parkinson's disease (PD) have suggested a role for ubiquitin-proteasome dysfunction and aberrant protein degradation in this disorder. Inasmuch as oxidative stress has also been implicated in PD, the present study examined transcriptional changes mediated by the Parkinsonism-inducing neurotoxins 6-hydroxydopamine (6-OHDA) and 1-methyl-4-phenylpyridinium (MPP⁺) in a dopaminergic cell line. Microarray analysis of RNA isolated from toxin treated samples revealed that the stress-induced transcription factor CHOP/Gadd153 was dramatically up-regulated by both 6-OHDA and MPP⁺. Treatment with 6-OHDA also induced a large number of genes involved in endoplasmic reticulum stress and unfolded protein response (UPR) such as ER chaperones and elements of the ubiquitin-proteasome system. Reverse transcription-PCR, Western blotting, and immunocytochemical approaches were used to quantify and temporally order the UPR pathways involved in neurotoxin-induced cell death. 6-OHDA, but not MPP⁺, significantly increased hallmarks of UPR such as BiP, c-Jun, and processed Xbp1 mRNA. Both toxins increased the phosphorylation of UPR proteins, PERK and eIF2 α , but only 6-OHDA increased phosphorylation of c-Jun. Thus, 6-OHDA is capable of triggering multiple pathways associated with UPR, whereas MPP⁺ exhibits a more restricted response. The involvement of UPR in these widely used neurotoxin models supports the role of ubiquitin-proteasome pathway dysfunction in PD.

Parkinson's disease (PD)¹ involves an irreversible degeneration of the dopaminergic nigrostriatal pathway, resulting in marked impairments of motor control. Although the etiology of PD remains unknown, both genetic and environmental factors appear to play a role. For example, three genes and several putative loci have been identified (1), including two autosomal dominant mutations of the α -synuclein gene, that were linked to rare familial early-onset PD (2, 3). α -Synuclein was subse-

quently shown to be the major component of Lewy bodies, the hallmark inclusion of PD (4). Parkin, a second gene with mutations associated with PD (5), has been shown to be an ubiquitin-protein isopeptide ligase (6). Loss of Parkin activity is linked to endoplasmic reticulum (ER) stress and unfolded protein response (UPR; Refs. 7 and 8). Finally, a missense mutation in the gene encoding ubiquitin C-terminal hydrolase L1 is also associated with rare cases of PD (9). Thus, aggregation of α -synuclein together with defects in the ubiquitin pathway support the notion that a dysfunctional ubiquitin-proteasome system in which aberrant proteins are not cleared may play a major role in PD. The role of proteasomal impairment has been further emphasized by recent reports that pharmacological inhibition of proteasome function leads to selective degeneration of dopaminergic neurons in culture (10) as well as *in vivo* (11). In particular, cell death was associated with increased cytoplasmic levels of α -synuclein and ubiquitin, as well as the formation of inclusion bodies (10, 11). Taken together, accumulating genetic and molecular evidence suggests that defects in ER and ubiquitin-proteasomal processing contribute to the pathogenesis of PD.

Because PD is largely restricted to dopaminergic neurons and because dopamine is easily oxidized *in vitro* and *in vivo* to a variety of neurotoxic metabolites, dopamine itself is considered a major factor in this disorder. For example, dopamine is readily oxidized to highly cytotoxic quinone molecules via at least three different enzymatic pathways (for review see Ref. 12). Moreover, in the presence of transition metals and hydrogen peroxide, dopamine can be converted to 6-OHDA (for review see Ref. 13), a highly potent endogenous neurotoxin widely used to create animal models of PD (13). Both 6-OHDA and other dopamine quinone derivatives have been found in post-mortem Parkinsonian brains (14–16), a finding that, together with the extensive studies documenting 6-OHDA-induced nigral degeneration, underscores the role dopamine plays in its own demise.

Similarly, another PD mimetic, N-methyl-4-phenyl-1,2,3,6-tetrahydropyridine (MPTP) or its active derivative, MPP⁺, is also thought to induce oxidative stress and impair energy metabolism (for review see Ref. 17). The original finding that human exposure to MPTP results in PD (18) has been replicated in various animal models including non-human primates (for review see Ref. 17). Thus, both 6-OHDA and MPP⁺ have been shown to produce reactive oxygen species and to inhibit mitochondrial complex I, as well as to mimic many behavioral, pharmacological, and pathological symptoms of this disorder (for review see Refs. 13, 17, and 19). Despite these parallels, the molecular mechanisms by which these neurotoxins kill cells remain unclear. Further, their relevance to emerging genetic and pharmacological models investigating ubiquitin-proteasome pathway dysfunction and protein aggregation has yet to be studied.

* This work was supported by NIH Grant NS39084 and Department of Defense Grant DAMD170110777. The costs of publication of this article were defrayed in part by the payment of page charges. This article must therefore be hereby marked "advertisement" in accordance with 18 U.S.C. Section 1734 solely to indicate this fact.

† To whom correspondence should be addressed: Anatomy and Neurobiology Department, Washington University School of Medicine, Box 8108, 660 S. Euclid Ave., St. Louis, MO 63110. Tel.: 314-362-7087; Fax: 314-362-3446; E-mail: omalleyk@peg.wustl.edu.

¹ The abbreviations used are: PD, Parkinson's disease; 6-OHDA, 6-hydroxydopamine; MPP⁺, 1-methyl-4-phenylpyridinium; UPR, unfolded protein response; RT, reverse transcription; ER, endoplasmic reticulum; MPTP, N-methyl-4-phenyl-1,2,3,6-tetrahydropyridine; PBS, phosphate-buffered saline; PERK, PKR-like ER kinase; SAPK, stress-activated protein kinase; JNK, c-Jun N-terminal kinase; ANOVA, analysis of variance; TH, tyrosine hydroxylase; eIF, eukaryotic initiation factor.

Previous results from this laboratory and others have demonstrated that 6-OHDA and MPP⁺ trigger morphologically distinct forms of cell death in the dopaminergic cell line MN9D and mouse primary mesencephalic cultures (13, 20, 21). Markers of apoptosis such as chromatin condensation and caspase-3 cleavage are widespread in cells treated with 6-OHDA, but not with MPP⁺. Despite the different forms of cell death induced by either toxin, both types of cell death seem to be dependent on *de novo* protein synthesis (22, 23). However, few studies of gene expression in 6-OHDA or MPP⁺-induced dopaminergic cell death models have been done. Presumably, this is a result of the scarcity and heterogeneity of the tissue involved as well as the technical limitation in analyzing a few genes at a time. Thus, at present, there is no information about the coordinated patterns of gene expression involved in 6-OHDA or MPP⁺ toxicity.

To unravel biological processes occurring in response to 6-OHDA and MPP⁺, we used microarray analysis of RNA isolated from the dopaminergic cell line MN9D (24) as a starting point to identify possible pathways induced by these Parkinsonian mimetics. These cells have been shown to mimic many aspects of the dopaminergic cell type from which they were immortalized (20–25). Capitalizing on the homogeneity and similarity in response of MN9D cells, the present study used microarray results, in addition to RT-PCR, Western blotting, and immunocytochemical approaches, to reveal that 6-OHDA triggers three separate signaling pathways associated with ER stress and UPR, whereas MPP⁺ seems to only involve one such signaling pathway. The unexpected identification of UPR induction in these models of dopaminergic cell death increases our understanding of how they may function to mimic the disease state and supports the theory that aberrations in the ubiquitin-proteasome pathway play an important role in PD.

MATERIALS AND METHODS

Cell Cultures—For primary cultures, the ventral mesencephalon was removed from embryonic day 14 CF1 murine embryos (Charles River Laboratories, Wilmington, MA) as described previously (21). Briefly, tissues were mechanically dissociated, incubated with 0.25% trypsin and 0.05% DNase in PBS for 20 min at 37 °C, and further triturated using a constricted Pasteur pipette. All plates were pre-coated overnight at room temperature with 0.5 mg/ml poly-D-lysine (Sigma) followed by 2.5 µg/ml laminin (BD Biosciences, San Jose, CA) for 2 h at 37 °C. Cells were maintained in serum-free Neurobasal medium (Invitrogen) supplemented with 1× B27 supplement (Invitrogen), 0.5 mM L-glutamine (Sigma), and 0.01 µg/ml streptomycin plus 100 units of penicillin. Half of the culture medium was replaced with fresh Neurobasal medium on the third and fifth day following plating. All experiments were conducted after 6 days *in vitro*.

MN9D cells were plated on dishes coated with 0.5 mg/ml poly-D-lysine for 1 h at 37 °C and then rinsed with sterile H₂O. Cells were maintained in Iscove's Dulbecco's modified Eagle's medium with 10% fetal bovine serum in an incubator with 10% CO₂ at 37 °C. Cells were switched to serum-free Iscove's Dulbecco's modified Eagle's medium/F-12 supplemented with 1× B27 prior to addition of experimental agents.

Cycloheximide Treatment and Determination of Cell Viability—MN9D cells were plated at a density of 40,000 cells/well in 24-well plates and treated after 3 days. One µg/ml cycloheximide (Calbiochem, La Jolla, CA) was added either immediately prior to, or at times following, addition of 100 µM 6-OHDA with ascorbic acid (dissolved in boiled water; Sigma) or 75 µM MPP⁺ (Sigma). After 48 h, cell survival was assessed using the 3-(4,5-dimethylthiazol-2-yl)-2,5-diphenyltetrazolium bromide reduction assay as previously described (22).

Microarray Analysis—MN9D cells were plated at a density of 200,000 cells/well in six-well plates. After 3 days, cells were treated with 75 µM 6-OHDA or 75 µM MPP⁺, or left untreated for control comparisons. Total RNA was isolated after 9 h of neurotoxin treatment using an RNeasy kit (Qiagen, Valencia, CA) according to the protocol from the manufacturer. Equal amounts of total RNA from three independent neurotoxin treatments were pooled together for each GeneChip hybridization experiment. Two separate GeneChip hybridizations of

pooled, treated, and control RNA were performed, representing six independent experiments. A minimum of 20 µg/sample of total RNA was sent to the Alvin J. Siteman Cancer Center GeneChip Core Facility (Washington University, St. Louis, MO) for generation of labeled cRNA target and hybridization against Affymetrix Murine Genome U74Av2 GeneChip arrays (Santa Clara, CA) using standard protocols (pathbox.wustl.edu/~mgacore). Data were analyzed by Affymetrix Microarray Suite version 5.0, as well as Spotfire Decision Site for Functional Genomics (Somerville, MA). For those transcripts designated both "present" and "increasing" in each replicate by the software, a threshold of an average signal log ratio greater than 0.5 (~1.5-fold change) was set. Transcripts for which signal was less than 3% of the maximum signal were filtered out.

Reverse Transcription-PCR—MN9D cells were plated and treated exactly as described for microarray experiments. Total RNA was extracted after 1, 3, 6, 9, and 12 h. Primers to 18 S ribosomal RNA (26) were used to standardize amounts of RNA in each sample. RNA was reverse transcribed using gene-specific reverse primers, and resulting cDNAs were PCR-amplified. PCR primer sequences used were: CHOP (+) and CHOP (−) described in Ref. 27, BiP/Fwd (TGACTGGAATTC-CTCCTGCT) and BiP/Rev (AGTCTTCAATGTCCGCATCC), c-jun/Fwd (GCTGAAGTGCATAGCCAGAA) and c-jun/Rev (CTTGATCCGCTCCT-GAGACT), and Xbp1/Fwd (TAGAAAGAAAGCCCGGA TGA) and Xbp1/Rev (CTCTGGGGAAGGACATTGTA). PCR products were resolved on a 4% PAGE gel and analyzed with Vistra Green (Amersham Biosciences) detection and quantitative fluorimaging.

Western Blot Analysis—For MN9D Western blots, cells were plated and treated exactly as described for microarray experiments. For primary culture Western blots, 600,000 cells/well were plated in six-well plates and treated on the 6th day *in vitro* with 40 µM 6-OHDA or 1 µM MPP⁺ (21). MN9D lysates were taken at 1, 3, 6, 9, and 12 h, and primary lysates were taken at 6 and 12 h. Cells were washed once with PBS and harvested in ice-cold radioimmune precipitation assay buffer (150 mM NaCl, 1% Nonidet P-40, 0.5% NaDoc, 0.1% SDS, 50 mM Tris, pH 8.0) with protease inhibitor mixture (Roche, Mannheim, Germany) and placed on ice for 30 min. Insoluble cell debris was removed by centrifugation, and the protein concentration of cell lysates was determined by the Bio-Rad protein assay. Equal amounts of protein were run on SDS-PAGE gels and then transferred to polyvinylidene difluoride membranes (Bio-Rad). Mouse monoclonal antibody against CHOP/Gadd153 (1:100) and goat polyclonal antibodies against Hsp60 (1:500) and BiP/Grp78 (1:125) were purchased from Santa Cruz Biotechnologies (Santa Cruz, CA). Rabbit polyclonal antibodies against cleaved caspase-3, phospho-c-Jun, phospho-eIF2α, and phospho-PERK (all 1:1,000) were purchased from Cell Signaling Technologies (Beverly, MA). After incubation with appropriate primary and horseradish peroxidase-conjugated secondary antibodies (anti-mouse 1:5000, Sigma; anti-goat 1:5000, Jackson Immunoresearch, West Grove, PA; or anti-rabbit 1:2000, Cell Signaling Technologies), specific protein bands were detected and analyzed by enhanced chemiluminescence substrate detection (ECL Plus; Amersham Biosciences) and quantitative fluorimaging.

Immunocytochemistry—MN9D cells were plated at a density of 300,000 cells/well on a four-well chamber slide. Twelve hours after plating, cells were treated with 75 µM 6-OHDA or 75 µM MPP⁺ and fixed 12 h later with 4% paraformaldehyde in PBS. Primary culture cells were plated at a density of 100,000 cells/35-mm microwell plate (1.25 × 10⁵ cells/mm²; MatTek Corp., Ashland, MA). On day 6 *in vitro*, cells were treated with 40 µM 6-OHDA or 1 µM MPP⁺, and fixed after 12, 18, or 24 h with 4% paraformaldehyde in PBS. Cultures were double-stained with either mouse monoclonal anti-CHOP (1:300) or rabbit polyclonal anti-phospho-c-Jun (1:500), together with rabbit polyclonal (1:500; Pel-Freez, Rogers, AR) or mouse monoclonal (1:2,500; Immunostar, Hudson, WI) antibodies against the dopaminergic neuron marker TH, respectively. Secondary antibodies conjugated with Cy3 (anti-mouse and anti-rabbit 1:300) and Alexa488 (anti-mouse 1:500; anti-rabbit 1:2000) were used. Cells were imaged using an Olympus Fluoview confocal microscope.

Statistics—GraphPad Prism software (San Diego, CA) was used for statistical analysis. The significance of effects between control and drug conditions was determined by one-way ANOVA as indicated and *post hoc* Dunnett's multiple comparison tests (GraphPad Prism software).

RESULTS

Cell Death Induced by 6-OHDA and MPP⁺ Is Blocked by Inhibition of Macromolecular Synthesis—Previous studies have characterized 6-OHDA-induced cell death as a caspase-

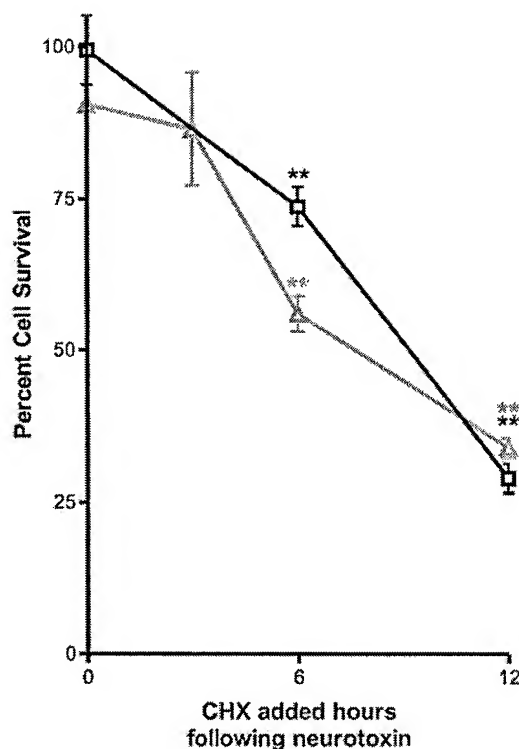


FIG. 1. New protein synthesis is required for MPP⁺ and 6-OHDA-induced cell death. MN9D cells were treated with 100 μ M 6-OHDA (squares) or 75 μ M MPP⁺ (triangles). One μ g/ml cycloheximide (CHX) was added either immediately prior to or at various times following neurotoxin addition. Cell survival was determined by 3-(4,5-dimethylthiazol-2-yl)-2,5-diphenyltetrazolium bromide assay and expressed as a percentage of survival compared with control cultures treated with cycloheximide alone. Values represent mean \pm S.E., $n = 4$. **, $p < 0.01$ compared with control (one-way ANOVA with post-hoc Dunnett's multiple comparison test). Error bars of less than 2% are buried in the symbol.

dependent, apoptotic process, whereas MPP⁺-induced cell death can occur independent of caspase activation, and without canonical markers of apoptosis (13, 20, 21, 28). Some forms of apoptotic and non-apoptotic cell death require *de novo* synthesis of cell death proteins (29, 30), whereas others do not (31, 32). To determine whether 6-OHDA- or MPP⁺-induced cell death require *de novo* macromolecular synthesis, cultures were treated with the protein synthesis inhibitor cycloheximide. Addition of 1.0 μ g/ml cycloheximide together with 100 μ M 6-OHDA or 75 μ M MPP⁺ provided significant protection. In contrast, delaying addition of cycloheximide following neurotoxin treatment resulted in increasing cell death in a time-dependent manner (Fig. 1). These data indicate that, although 6-OHDA induces an apoptotic form of cell death and MPP⁺ does not, both types of cell death require *de novo* protein synthesis. Therefore, it may be possible to identify changes in gene expression associated with the cell death process.

Microarray Analysis Identifies Distinct Changes in Gene Expression following 6-OHDA and MPP⁺ Treatment—Microarray analysis was used to examine the expression profile of a large number of transcripts. Out of the ~12,000 genes and expressed sequence tags represented on the MG-U74Av2 GeneChip, 4,304 (~35% of total) were defined as "present" by the microarray analysis software for MPP⁺-treated samples. Similarly, 4,580 (~37% of total) were defined as present for 6-OHDA-treated samples. Transcripts were subsequently grouped by individual toxin treatment, or by both 6-OHDA and MPP⁺ (Fig. 2). Notably, 6-OHDA treatment affected almost three times as many transcripts as MPP⁺. Specifically, 153 transcripts in-

creased in response to 6-OHDA, whereas only 55 transcripts increased in response to MPP⁺. Results for decreasing transcripts were similar (data not shown). Both neurotoxins induced a number of the same transcripts, with 39 of the 55 transcripts induced by MPP⁺ also induced by 6-OHDA (Table I). These included genes involved in cell cycle and/or differentiation, signaling, stress, and transcription factors, indicating possible common cell death mechanisms. The most highly induced transcript in response to either treatment was that to the stress protein CHOP/Gadd153. 6-OHDA also induced a large number of transcripts that were unchanged by MPP⁺ treatment, including molecular chaperones and other genes involved in protein folding, trafficking, and the ubiquitin-proteasome pathway (Table II). These results support previous findings showing that MPP⁺ and 6-OHDA promote distinct yet overlapping programs of cell death.

CHOP Is Induced in Response to 6-OHDA and MPP⁺—To confirm the microarray findings that CHOP mRNA was up-regulated by 6-OHDA and MPP⁺ in MN9D cells, RT-PCR was performed (Fig. 3A). 6-OHDA induced a large and rapid induction of CHOP mRNA that peaked between 6 and 9 h. MPP⁺ induction of CHOP mRNA lagged behind that of 6-OHDA, but continued to increase for at least 12 h (Fig. 3, A and C). These data are consistent with the GeneChip results from a 9-h time point showing greater induction with 6-OHDA than with MPP⁺ (Fig. 2 and Table I). Western blotting of MN9D total cell lysates confirmed that levels of CHOP protein were also increasing (Fig. 3, B and C). Again, 6-OHDA induced a larger and more rapid increase in protein expression than did MPP⁺ (Fig. 3C). To visualize CHOP induction *in situ* (Fig. 3D), treated cells were fixed, stained, and imaged using confocal microscopy. Control cultures had dim, diffuse staining, whereas both 6-OHDA and MPP⁺ treated cells showed intense nuclear staining. This localization is consistent with the role of CHOP as a transcription factor. Together, these results confirm and extend the GeneChip findings that toxin treatment of dopaminergic cells leads to an up-regulation of CHOP mRNA and protein levels.

RT-PCR Reveals Markers of Unfolded Protein Response Are Up-regulated by 6-OHDA and MPP⁺ Treatment—CHOP is up-regulated by a variety of cellular stresses including ER stress (27, 33–35). Following confirmation of CHOP induction, further analysis of GeneChip results revealed a pattern of induction of other stress-induced genes including many involved in UPR (Fig. 2, Tables I and II). These included molecular chaperones such as BiP/Grp78 and UPR-induced transcription factors other than CHOP (Atf4 and Xbp1). To examine the role that UPR may play in 6-OHDA and MPP⁺ toxicity, induction of these transcripts was verified by RT-PCR (Fig. 4, A and B). BiP is an ER-resident chaperone protein central to UPR (36). Levels of BiP mRNA were increased greater than 2-fold over control from 6 to 12 h following 6-OHDA exposure. BiP expression, however, decreased slightly in response to MPP⁺ exposure over 12 h. These results were consistent with GeneChip results at 9 h for both 6-OHDA and MPP⁺ (Table II). Although not specific to ER stress, activation of the c-Jun N-terminal kinase/stress-activated protein kinase pathway (JNK/SAPK) occurs during UPR (37, 38). Expression of c-Jun mRNA was increased rapidly by 6-OHDA and then maintained at levels 5–6-fold that of control from 3 to 12 h following exposure. MPP⁺ treatment resulted in a rapid induction of c-Jun mRNA to 3-fold that of control at 1 h, identical to exposure to 6-OHDA. However, MPP⁺ induction of c-Jun mRNA was not sustained and returned to control levels by 9 h.

Another feature of the UPR pathway is the non-conventional removal of 26 base pairs of Xbp1 mRNA by the ER membrane

FIG. 2. Microarray analysis reveals both common and distinct transcriptional changes induced by 6-OHDA and MPP⁺. Total RNA from MN9D cells treated with 6-OHDA or MPP⁺ in addition to untreated control was used for Affymetrix MG-U74Av2 GeneChip array probe hybridization. Data were analyzed by Affymetrix Microarray Suite version 5 as well as Spotfire Decision Site for Functional Genomics. Transcriptional changes were defined as described in the text. Large plot shows known genes induced by 6-OHDA or MPP⁺ treatment plotted as average-fold induction on the x axis and y axis, respectively, with a scale of log₂. Several genes of interest have been labeled (see Tables I and II for abbreviations used). Independent of their position on the plot, genes were grouped according to those induced by 6-OHDA but not induced by MPP⁺ (green squares), those induced by MPP⁺ but not induced by 6-OHDA (gray triangles), or those induced by both 6-OHDA and MPP⁺ (blue circles). Inset shows all ~12,000 genes represented on the Affymetrix MG-U74Av2 GeneChip. Red points represent the 169 increasing genes identified as described in text.

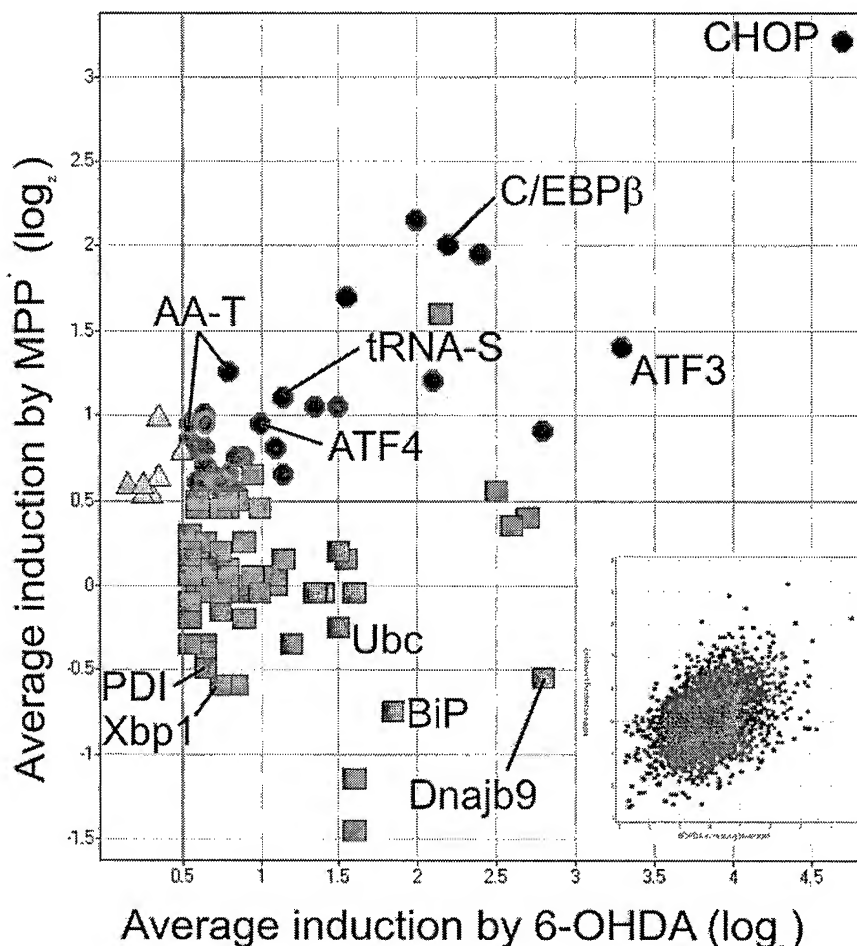


TABLE I
Genes increased by both 6-OHDA and MPP⁺

Table lists 18 of 39 transcripts increased by both 6-OHDA and MPP⁺.

Gene symbol	Gene name	Change	
		6-OHDA	MPP ⁺
		fold	
<i>Gadd153</i>	CHOP/Gadd153	26.0	9.2
<i>Atf3</i>	Activating transcription factor 3	9.8	2.6
<i>Cebpb</i>	CCAAT/enhancer-binding protein C/EBP-β	4.6	4.0
<i>Sqstm1</i>	Sequestosome 1	7.0	1.9
<i>Myd116</i>	Myeloid differentiation primary response gene 116	4.3	2.3
<i>Gtpbp2</i>	GTP-binding protein 2	2.9	3.2
<i>Lbcl1</i>	Lymphoid blast crisis-like 1 (cell growth and maintenance)	2.5	2.1
<i>Cars</i>	Cysteinyl-tRNA synthetase	2.2	2.1
<i>Slc1a4</i>	Neutral amino acid transporter	1.7	2.4
<i>Atf4</i>	Activating transcription factor 4	2.0	1.9
<i>Gas5</i>	Growth arrest-specific 5	2.1	1.7
<i>Eif4ebp1</i>	Eukaryotic translation initiation factor 4E binding protein 1	1.6	2.0
<i>Slc7a5</i>	Solute carrier family 7 cationic amino acid transporter	1.5	1.9
<i>Glyt1</i>	Glycine transporter 1	1.6	1.7
<i>Clcn4</i>	Chloride intracellular channel 4 mitochondrial	1.5	1.8
<i>Clcn3</i>	Chloride channel 3	1.8	1.5
<i>Wars</i>	Tryptophanyl-tRNA synthetase	1.6	1.6
<i>Hspa9a</i>	Heat shock protein cognate 74 (mitochondrion)	1.6	1.5

resident protein, Ire1α/β, under conditions of ER stress (39, 40). Moreover, levels of unprocessed Xbp1 mRNA are also increased by ER stress. In response to 6-OHDA but not MPP⁺, Xbp1 was induced almost 2-fold according to the GeneChip analysis (Fig. 2, Table II). To determine whether Xbp1 mRNA was processed, primers flanking the excised portion of Xbp1 mRNA were used to reveal a shift in size of the RT-PCR product

(Fig. 4A). As indicated in Fig. 4B, 6-OHDA produced a large, transient induction of processed Xbp1 mRNA peaking at 3–6 h and returning to near control levels after 12 h. In contrast, MPP⁺ treatment resulted in a sustained inhibition of Xbp1 mRNA processing from 3 to 12 h.

Western Blotting Reveals Markers of Unfolded Protein Response Are Up-regulated by 6-OHDA and MPP⁺ Treatment—

TABLE II
Genes increased by 6-OHDA onlyTable lists 21 of 114 transcripts increased by 6-OHDA, but not by MPP⁺.

Gene symbol	Gene name	Change	
		6-OHDA	MPP ⁺
		fold	
<i>Dnajb9</i>	DNA j protein b9	7.0	0.7
<i>Herpud1</i>	ER stress-inducible ubiquitin-like domain member 1	6.5	1.3
<i>Hmox1</i>	Heme oxygenase decycling 1	5.7	1.5
<i>Hspa5</i>	Bip/Grp78	3.0	0.5
<i>Ubc</i>	ubiquitin C	2.8	0.8
<i>Bag3</i>	Bcl2-associated athanogene 3 (cytosol anti-apoptotic)	2.6	1.0
<i>Tra1</i>	Tumor rejection antigen gp96 (chaperone calcium binding)	2.3	0.8
<i>Sec23b</i>	SEC23B <i>Saccharomyces cerevisiae</i> (ER intracellular protein trafficking)	2.1	1.0
<i>Por</i>	P450 cytochrome oxidoreductase	2.1	1.0
<i>Txnrd1</i>	Thioredoxin reductase 1	1.9	1.0
<i>Spc18</i>	Signal peptidase complex 18-kDa	1.9	0.9
<i>Arhb</i>	Aplysia Ras-related homolog B RhoB	1.8	1.0
<i>Xbp1</i>	X-box-binding protein 1	1.7	0.7
<i>Hsc70t</i>	Heat shock protein cognate 70 testis	1.7	0.9
<i>Sec23a</i>	SEC23A <i>S. cerevisiae</i> (ER intracellular protein trafficking)	1.6	1.0
<i>Ppib</i>	Peptidylprolyl isomerase B	1.6	1.0
<i>Grp58</i>	grp58 kDa (protein-disulfide isomerase)	1.6	0.7
<i>Psmc4</i>	Proteasome 26 S subunit, non-ATPase, 4	1.5	1.1
<i>S100a10</i>	Calcium-binding protein A11 calgizzarin	1.5	0.9
<i>Sec61g</i>	SEC61 gamma subunit <i>S. cerevisiae</i>	1.5	0.9
<i>Uch11</i>	Ubiquitin C-terminal hydrolase L1	1.5	1.1

Induction of the UPR pathway triggers not only transcriptional changes, but also involvement of protein kinase signaling pathways. One such pathway is that of JNK/SAPK, activation of which leads to phosphorylation of c-Jun (37, 38). In addition to changes in c-Jun mRNA expression (Fig. 4, A and B), Western blot analysis using antibodies against phospho-c-Jun indicated that 6-OHDA administration increased phosphorylation of c-Jun ~6-fold over control levels at 9–12 h (Fig. 5, A and B). In contrast, treatment with MPP⁺ induced a transient increase of phosphorylated c-Jun at 3 h, returning to control levels by 6–9 h. These data are consistent with the RT-PCR results indicating a slight, early MPP⁺ mediated increase in c-Jun mRNA that was not sustained (Fig. 4, A and B). Taken together these results indicate that cellular responses to 6-OHDA led to the activation of the JNK/SAPK pathway.

Another consequence of UPR is translational attenuation caused by phosphorylation of eIF2 α by the ER membrane resident kinase PERK. Western blotting using antibodies against phospho-eIF2 α revealed that both 6-OHDA- and MPP⁺-mediated toxicity resulted in eIF2 α phosphorylation (Fig. 5, A and B). Specifically, MPP⁺ exposure induced a rapid, transient response, whereas 6-OHDA exposure resulted in sustained phosphorylation of eIF2 α from 3 to 12 h. The eIF2 α kinase PERK is itself activated by phosphorylation, and Western results indicated that MPP⁺ induced PERK phosphorylation in a profile almost identical to eIF2 α phosphorylation. In contrast, PERK phosphorylation induced by 6-OHDA exhibited delayed kinetics, staying at baseline levels for 3 h following treatment, and then rising 3-fold over the next 9 h. BiP protein levels showed a slight increase over 12 h with 6-OHDA treatment, but not with MPP⁺ (Fig. 5A), again consistent with both GeneChip and RT-PCR data. In accordance with previous reports that 6-OHDA induced apoptosis (20, 21), but MPP⁺ does not, activated caspase-3 was detected only in 6-OHDA-treated cultures (Fig. 5A). Collectively, these data reveal that many components of UPR, including multiple signaling pathways, were up-regulated in response to 6-OHDA toxicity. In contrast, treatment with MPP⁺ led to the up-regulation of some, but not all, markers of UPR. Thus, MPP⁺ may ultimately lead to dopaminergic cell death by a pathway that is at least partially independent of UPR.

6-OHDA, but Not MPP⁺, Induces Components of the UPR Pathway in Primary Mesencephalic Cultures—To determine

whether UPR induction could be observed in primary mesencephalic cultures following neurotoxin treatment, Western blot analysis and immunocytochemistry were performed. Similar to results from the dopaminergic MN9D cells, 6-OHDA increased levels of CHOP protein at 6 and 12 h (Fig. 6A). 6-OHDA also increased phosphorylation of eIF2 α and c-Jun. In contrast, none of the markers seen in the dopaminergic cell line were up-regulated in mesencephalic cultures treated with MPP⁺. Neither 6-OHDA nor MPP⁺ induced significant changes in levels of BiP protein over 12 h (data not shown).

Immunostaining of primary cultures with CHOP and phospho-c-Jun antibodies allowed individual dopaminergic neurons to be examined via co-staining with TH. 6-OHDA-treated cultures displayed intense nuclear staining of CHOP in both dopaminergic neurons as well as in many other cell types. Cultures treated with MPP⁺ did not appear different from controls in overall expression of CHOP, nor was CHOP induction detected in dopaminergic neurons over a 24-h period. Similarly, increased expression of phospho-c-Jun was widespread with 6-OHDA treatment in both dopaminergic and non-dopaminergic neurons, whereas there was no obvious change in phosphorylation of c-Jun following MPP⁺ administration. Taken together, these results suggest that MPP⁺ can induce a partial UPR response in the MN9D cell line but not in cultured dopaminergic neurons. In contrast, 6-OHDA induces a broad spectrum of UPR responses in both MN9D cells as well as in dissociated dopaminergic neurons. Thus, these cells will serve as a useful model in determining the temporal and molecular events associated with 6-OHDA neurotoxicity.

DISCUSSION

Accumulating evidence suggests that ER stress induced by aberrant protein degradation plays a role in PD. Beginning with a functional genomics approach to identify transcriptional alterations in a well characterized model of 6-OHDA and MPP⁺ toxicity, the present study identified numerous changes in genes associated with UPR. Notably, a major target of the UPR pathway, the transcription factor CHOP, was dramatically up-regulated at both the mRNA and protein levels by either 6-OHDA or MPP⁺. Moreover, 6-OHDA activated numerous other markers of UPR including BiP, splicing of Xbp1 mRNA, the JNK/SAPK pathway, as well as proteins involved in the

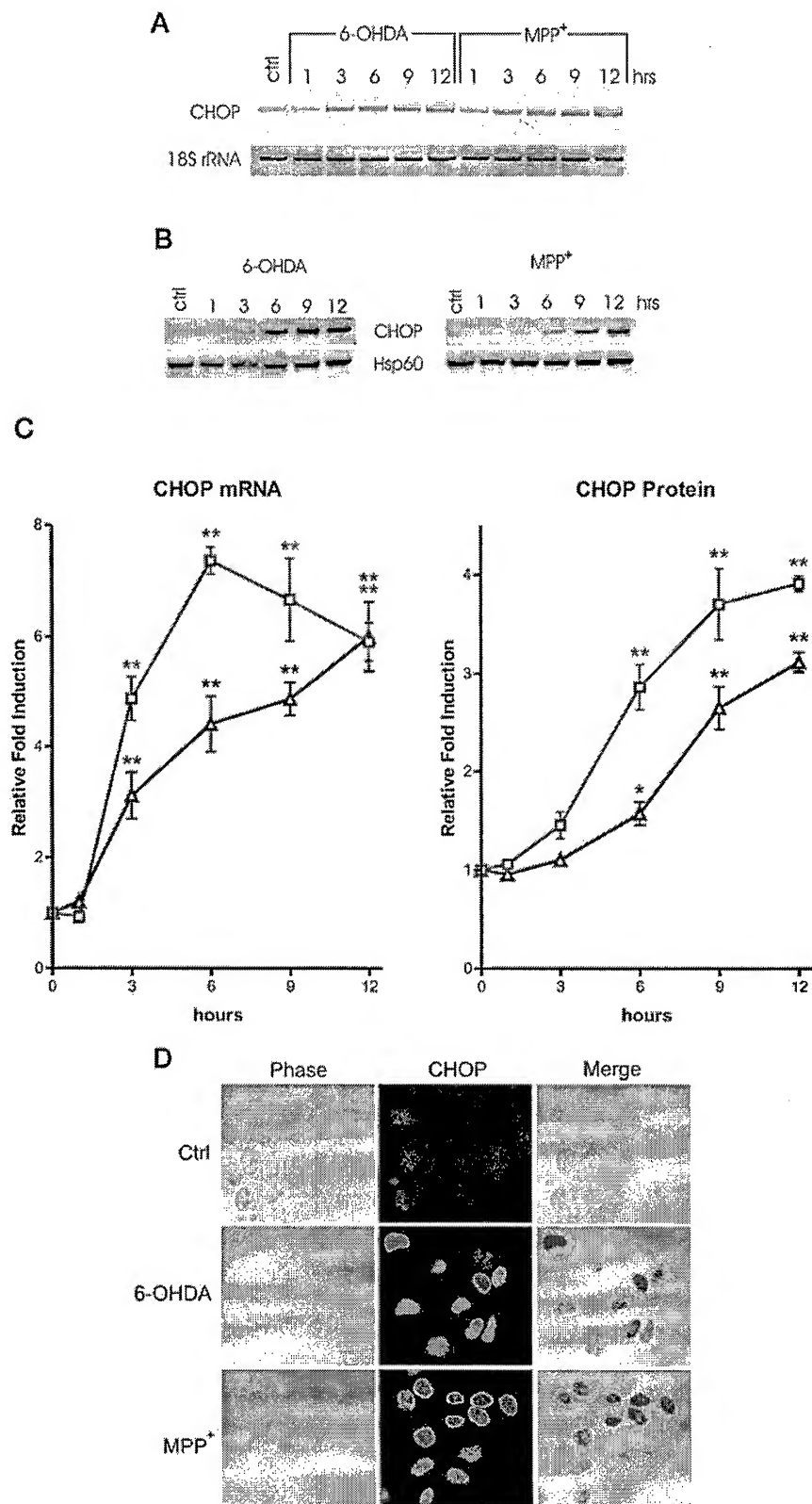


FIG. 3. CHOP is up-regulated following 6-OHDA and MPP⁺ administration. Treatment with 6-OHDA and MPP⁺ increased levels of CHOP mRNA isolated from MN9D cells as detected by RT-PCR (A) and levels of CHOP protein isolated from MN9D cells as detected by Western blot analysis (B). Equivalent loading was monitored by 18 S rRNA and Hsp60, respectively. C, quantification of CHOP mRNA and protein induced by 6-OHDA (squares) and MPP⁺ (triangles) was performed as described in text. Values represent mean \pm S.E. of triplicate RT-PCRs and Western blots. *, $p < 0.05$; **, $p < 0.01$ compared with untreated control (one-way ANOVA with post-hoc Dunnett's multiple comparison test). Error bars of less than 2% are buried in the symbol. D, MN9D cells were fixed after 12 h of neurotoxin treatment and stained with an antibody against CHOP. Left panels are phase bright images showing the morphology of MN9D cells. Middle panels show CHOP immunostaining. Nuclear localization of CHOP can be observed in the merged right panels.

A

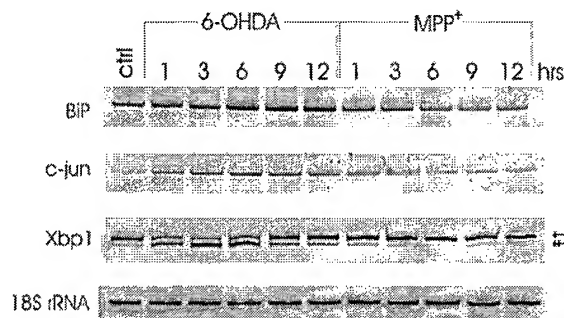
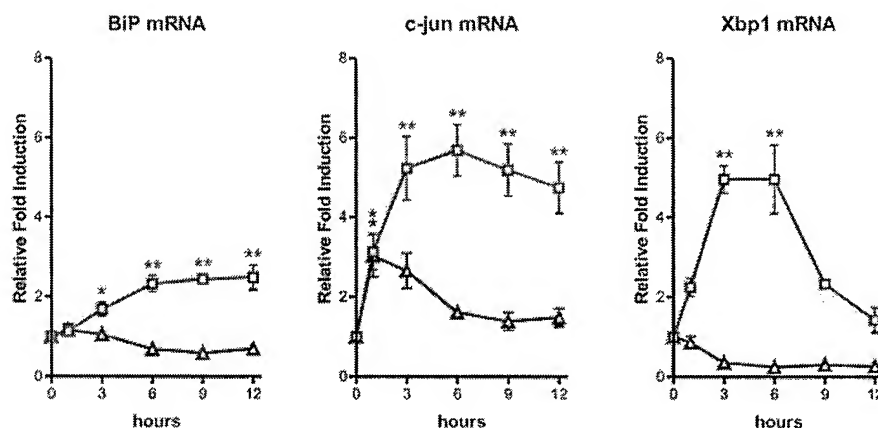


FIG. 4. 6-OHDA, but not MPP⁺, induced transcriptional changes downstream of Ire1 α / β and ATF6 UPR pathways. A, total RNA was isolated from MN9D cells treated with 6-OHDA and MPP⁺ and used for reverse transcription and semiquantitative RT-PCR using primer pairs to BiP/Grp78, c-Jun, and Xbp1. RT-PCR products were separated on a 4% PAGE gel and visualized with Vistra Green staining. Equal loading was monitored by 18 S rRNA RT-PCR. Xbp1 RT-PCR resulted in two products representing the unprocessed (upper; single arrowhead) and processed (lower; double arrowhead) forms of Xbp1 mRNA. B, quantification of RT-PCR products induced by 6-OHDA (squares) and MPP⁺ (triangles) was performed as described in text. Values represent mean \pm S.E. of triplicate RT-PCRs. *, $p < 0.05$, **, $p < 0.01$ compared with untreated control (one-way ANOVA with post-hoc Dunnett's multiple comparison test). Error bars of less than 2% are buried in the symbol.

B



attenuation of translation such as PERK and eIF2 α . In contrast, MPP⁺ effects appeared restricted to events associated with PERK and eIF2 α phosphorylation. In confirmation of these cell line results, 6-OHDA also triggered UPR responses in primary cultures of dopaminergic neurons. Collectively these data emphasize that 6-OHDA and MPP⁺ induce distinct cell death responses. Inasmuch as 6-OHDA is widely used to create animal models of PD, the present findings further support the notion that ER stress and ubiquitin-proteasome dysfunction is associated with this disorder.

Biological Sequelae Associated with PD Mimetics—Oxidative stress and mitochondrial dysfunction have long been implicated in PD (41). Because of this, two neurotoxins exhibiting specificity toward dopaminergic neurons, 6-OHDA and MPP⁺, are commonly used to model nigral degeneration. 6-OHDA is a potent inducer of oxidative stress that can be endogenously converted from dopamine (13). Dopamine quinone derivatives including 6-OHDA have been found in post-mortem PD brains (14–16), implicating dopamine itself as a factor in this disorder. MPTP was originally identified because accidental human exposure led to PD (18, 42). MPTP, and its active metabolite MPP⁺, are also thought to induce oxidative stress in addition to inhibiting mitochondrial function (17). The discovery that mutations in α -synuclein (2, 3), parkin, and UCH-L1 (5, 9, 43, 44) are associated with PD led to the recognition that impaired protein degradation is also an important factor in this disorder. Mechanistically, however, it is still unclear what the common thread is among these seemingly disparate cellular responses.

The present study utilized gene expression profiling to assess thousands of genes to obtain a more detailed understanding of the molecular programs utilized by dopaminergic cells in response to 6-OHDA and MPP⁺. Two important outcomes from this study include the identification of a previously unsus-

pected link between these known oxidative stress inducers and aspects of ER stress/UPR, as well as the identification of at least a subset of common transcriptional changes associated with toxin-mediated events. The latter observation emphasizes the overlapping yet divergent nature of cell death in response to 6-OHDA versus MPP⁺.

Commonality in response to 6-OHDA and MPP⁺ is highlighted by the finding that the most highly induced transcript by either toxin was CHOP, a stress-induced transcription factor implicated in cell death (34, 45). The temporal and spatial up-regulation of CHOP was confirmed and extended by RT-PCR, Western blot analysis, and immunocytochemistry (Fig. 3). In support of the present findings, microarray analysis of MPP⁺-treated SH-SY5Y cells also resulted in an up-regulation of CHOP, albeit with a much later, more prolonged time course (46). Similarly, microarray analysis of the dopaminergic cell line, SN4741, revealed induction of stress indices following MPP⁺ treatment (47). To date, however, this is the first report that 6-OHDA up-regulates CHOP, and that it does so to a much greater extent than MPP⁺.

Additional transcripts identified via microarray analysis revealed that 6-OHDA induced a large number of genes that were not positively affected by MPP⁺, many of which were involved in protein folding, trafficking, or degradation (Table II). In contrast, the subset of genes induced by both drugs included amino acid transporters, tRNA-synthetases, ion channels, and stress-induced transcription factors (Table I). A small number of genes was induced by MPP⁺ but not 6-OHDA. These included Dnaja3, adaptor-related protein complex AP-3 β 1 subunit, and myelin transcription factor 1. Currently, the significance of these changes is unclear. Overall, MPP⁺-induced transcripts appeared to primarily represent a subset of genes induced by 6-OHDA.

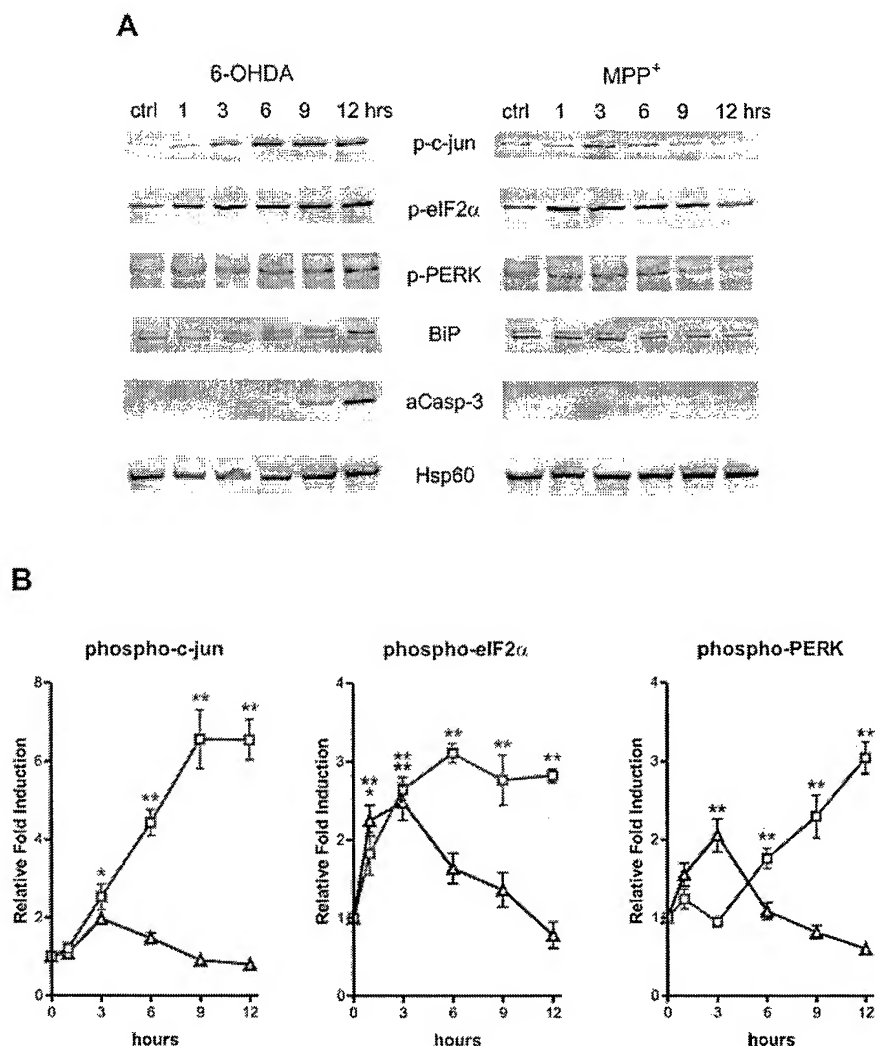


FIG. 5. 6-OHDA induced sustained phosphorylation of proteins associated with Ire1 α / β and PERK UPR pathways, whereas MPP⁺ induced only transient changes. Protein lysates were prepared from MN9D cells treated with 6-OHDA and MPP⁺. **A**, antibodies against the phosphorylated forms of c-Jun (p-c-jun), eIF2 α (p-eIF2 α), and PERK (p-PERK) were used for Western blot analysis. Additional antibodies were used to detect BiP, activated caspase-3 (aCasp-3), and Hsp60 as a protein loading control. **B**, quantification of phosphorylated proteins induced by 6-OHDA (squares) and MPP⁺ (triangles) was performed as described in text. Values represent mean \pm S.E. of triplicate Western blots. * p < 0.05; ** p < 0.01 compared with untreated control (one-way ANOVA with post-hoc Dunnett's multiple comparison test). Error bars of less than 2% are buried in the symbol.

UPR Signaling Pathways—Three signaling pathways have been associated with UPR that are triggered by the ER proteins, Ire1 α / β , ATF6, and PERK review (48). The Ire1 α / β pathway is thought to activate caspase-12, the JNK/SAPK pathway, as well as Xbp1 mRNA splicing (37, 39, 40, 49). Translocation of ATF6 to the nucleus leads to the up-regulation of Xbp1 as well as various ER chaperones (48, 50). Finally, in addition to transcriptional changes, ER stress/UPR can down-regulate protein translation through phosphorylation of eIF2 α via PERK kinase activity (48). Of interest, there is some redundancy in these cascades. For example, CHOP can be up-regulated by both the ATF6 and PERK pathways (50, 51). CHOP, as well as many chaperone proteins, contains a binding site called the ER stress element in its promoter region. In the nucleus, ATF6 binds to ER stress element sites activating CHOP transcription. In addition, CHOP contains a second site called the amino acid response element that is bound by the transcription factors ATF4 and C/EBP β . ATF4 is activated when eIF2 α is phosphorylated by PERK (48) or other eIF2 α kinases (52, 53). Thus, signaling through PERK also leads to the up-regulation of CHOP.

GeneChip analysis indicated that many of the genes induced by either MPP⁺ or 6-OHDA were increased to a similar extent. A notable exception, however, was that 6-OHDA induced CHOP 26-fold compared with 9-fold with MPP⁺ (Fig. 2, Table

I). Moreover, although both neurotoxins increased ATF4 and C/EBP β , only 6-OHDA increased Xbp1 mRNA levels (Fig. 2). These data are consistent with the notion that 6-OHDA triggered both ATF6 and PERK pathways leading to the dual activation of the CHOP promoter. Moreover, processing of Xbp1 mRNA, indicating activation of the Ire1 α / β pathway, was only observed with 6-OHDA. Although at present we have no clear evidence that caspase-12 is activated (data not shown), 6-OHDA but not MPP⁺ also dramatically up-regulated c-Jun mRNA (Fig. 4) and markedly increased phospho-c-Jun levels (Fig. 5). Taken together, it seems reasonable to propose that 6-OHDA is activating all three branches of the UPR signaling cascade, Ire1 α / β , ATF6, and PERK, whereas MPP⁺ is only activating the PERK branch. One possible model summarizing these results is shown in Fig. 7.

Additional support for this hypothesis comes from studies showing that eIF2 α can also be phosphorylated by other kinases such as GCN2 in response to amino acid starvation (52) or PKR in response to viral infection (53). Thus, phosphorylation of eIF2 α does not require activation of the entire UPR and can lead to induction of genes downstream of ATF4, but not ATF6 (50, 51). The present findings are consistent with the model that MPP⁺ triggers eIF2 α phosphorylation (Fig. 7) without involving ATF6 and Ire1 α / β activation. These data are remarkably similar to a recent report showing that arsenite

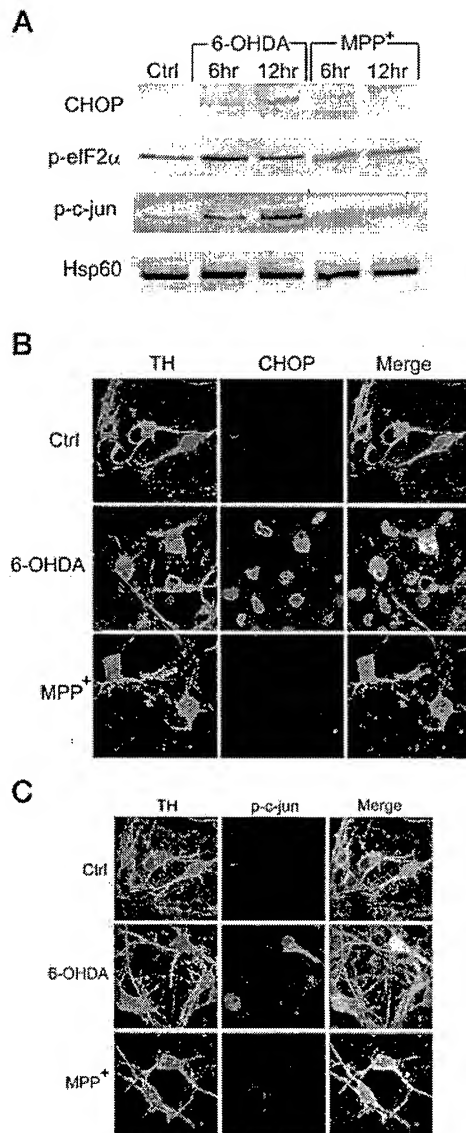


FIG. 6. 6-OHDA up-regulates CHOP in primary mesencephalic neurons. Protein lysates were prepared from primary mesencephalic cultures treated with 6-OHDA and MPP⁺. **A**, Western blot analysis of primary lysates was done using antibodies against CHOP, phosphorylated eIF2 α (*p-eIF2 α*), phosphorylated c-Jun (*p-c-jun*), and Hsp60 as a protein loading control. **B**, primary cultures treated for 18 h were fixed and stained for CHOP and TH. **C**, primary cultures treated for 12 h were fixed and stained for phospho-c-Jun and TH.

exposure of primary neuronal cells led to the up-regulation of CHOP expression without a concurrent activation of UPR (54). Thus, MPP⁺-mediated cell death parallels that described for amino acid starvation and/or toxin treatment.

6-OHDA- or MPP⁺-mediated Cell Death—Previously we and others have shown that, although 6-OHDA and MPP⁺ both generate oxidative stress, only 6-OHDA treatment resulted in activation of caspases and morphological changes associated with apoptosis (20, 21). Several lines of evidence from this laboratory suggest, however, that 6-OHDA does not mediate an intrinsic, mitochondrial dependent, apoptotic pathway. For example, overexpression of the anti-apoptotic protein, Bcl-2, did not attenuate 6-OHDA-induced cell death in either the MN9D cell line or in primary dopaminergic neurons (22, 25). Moreover, deletion of the pro-apoptotic Bcl-2 family member, Bax, did not rescue dopamine neurons from 6-OHDA toxicity (25),

nor was Bax protein translocated to the mitochondria in response to this toxin.² Finally, microarray analysis failed to detect up-regulation of any BH3-only family proteins thought to act upstream of the intrinsic mitochondrial pathway, even though downstream caspases were activated (Fig. 5A). Thus, these data support a model in which 6-OHDA activates apoptosis without involving the intrinsic mitochondrial pathway.

Another possibility is that 6-OHDA activates the extrinsic apoptotic pathway involving death receptors such as Fas and the induction of caspase-8. The extrinsic pathway can occur independent of *de novo* protein synthesis (32, 55, 56) as well as Bcl-2 family member expression (for review see Ref. 57). However, activation of the extrinsic pathway requires ligand-mediated death receptor multimerization, adaptor proteins such as FADD, as well as autoproteolysis of caspases-8 and -10 (for review see Ref. 58). In the case of 6-OHDA-induced apoptosis, utilization of the extrinsic pathway seems unlikely because it was dependent on new protein synthesis, known death-inducing ligands were not identified by microarray analysis, and so-called death receptors (Fas (APO-1, CD95), tumor necrosis factor receptor 1 (TNF-R1), TNF-related apoptosis-inducing ligand receptor I and II, etc.; Ref. 59) as well as Fas-associated death domain were not detected either. In contrast, a growing body of evidence indicates that ER stress can induce apoptosis independent of both extrinsic and intrinsic pathway factors requiring instead caspase-12 and caspase-9 (60, 61). Apoptosis mediated by 6-OHDA appears to have more characteristics in common with this alternative, non-mitochondrial, pathway, although the involvement of caspases-9 and -12 remains to be determined.

The present data as well as previous studies (20, 21) help to order and clarify the temporal events following neurotoxin treatment. Previous studies of primary dopaminergic neurons have shown that 6-OHDA induced an immediate increase (minutes) in reactive oxygen species (ROS) (21). The current findings suggest that following ROS generation 6-OHDA treatment quickly leads to the induction of c-Jun and processed Xbp1 mRNA (Fig. 4). These mRNAs are increased after 1 h and reach near maximal values by 3 h. Another early event is the phosphorylation of eIF2 α , which is also increased significantly at 1 h, peaks at 3 h, and then stays elevated for the next 9 h (Fig. 5). Presumably triggered by the aforementioned primary events, a distinct second wave of transcriptional responses occurs, exemplified by CHOP and BiP. The latter are unchanged at 1 h and then rise rapidly (Fig. 3, 4). Phosphorylation of c-Jun also occurs during this time (Fig. 5). Reflecting an earlier increase in levels of CHOP mRNA, increased CHOP protein is detected after 6 h (Fig. 3). In addition, phosphorylation of PERK is not detected until 6 h following 6-OHDA exposure (Fig. 5). The last event to occur in this study was the activation of caspase-3, which was barely detectable at 9 h and only increased significantly after 12 h (Fig. 5A). Previous studies have shown that the pan-caspase inhibitor benzyloxycarbonyl-Val-Ala-Asp-fluoromethylketone blocks 6-OHDA toxicity in MN9D cells (20) and that the pan-caspase inhibitor bocasparyl(Ome)-fluoromethylketone is similarly effective in cultured dopaminergic neurons (21). Thus, a broad, multiphasic program of transcriptional, translational, and post-translational events precedes 6-OHDA-induced dopaminergic cell death.

Following transient increases, MPP⁺-induced phospho-PERK, phospho-eIF2 α , and phospho-c-Jun levels all decreased to near control levels after 6–9 h of exposure, whereas these same proteins remained phosphorylated in response to

² W. A. Holtz and K. L. O'Malley, unpublished observation.

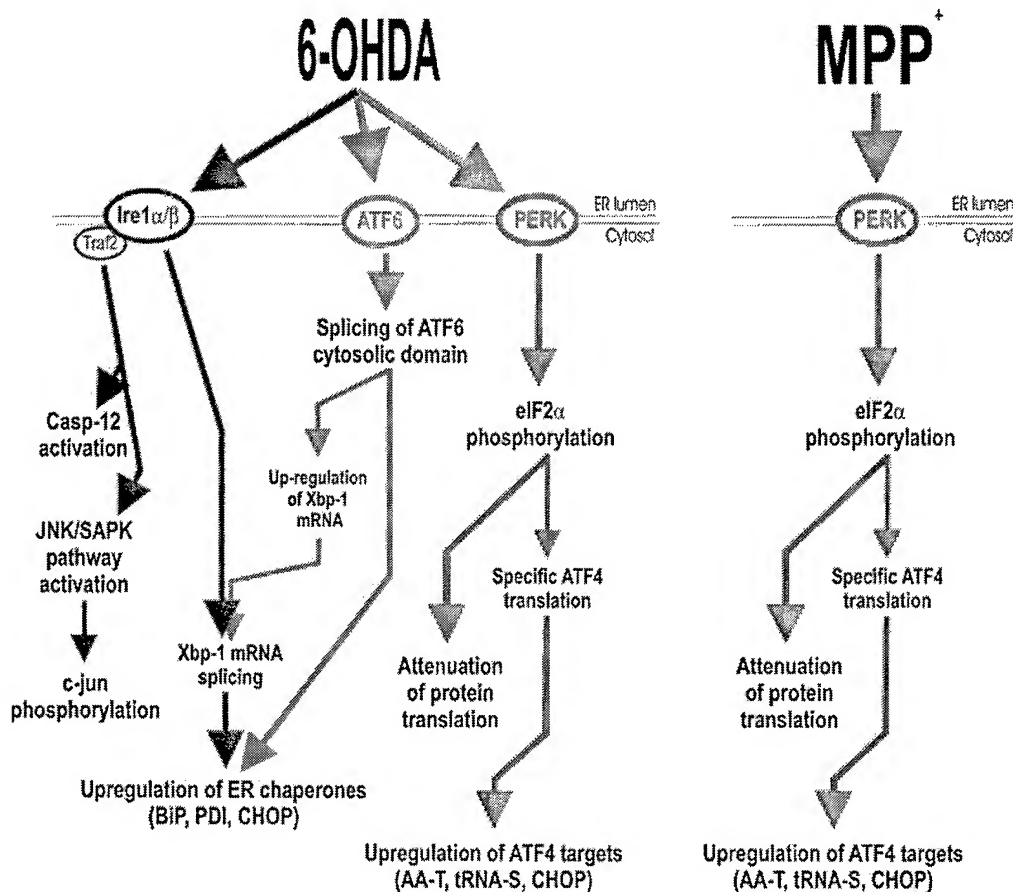


FIG. 7. 6-OHDA induces multiple targets of UPR, whereas MPP⁺ is restricted to the PERK pathway. The mammalian UPR consists of three ER membrane resident proteins (Ire1 α/β , ATF6, and PERK) that sense ER stress and activate the UPR pathway resulting in transcriptional changes and attenuation of protein translation. The current studies demonstrate that 6-OHDA induces all three arms of the UPR leading ultimately to the transcriptional changes first identified by microarray analysis. In contrast, MPP⁺ is restricted to phosphorylation of PERK and eIF2 α , resulting in up-regulation of a subset of genes induced by 6-OHDA.

6-OHDA. Why then are MPP⁺ mediated changes transient? One possible explanation is that, although both toxins initially trigger the same response as a result of oxidative stress, this response diverges as MPP⁺ more effectively depletes cellular energy. Conceivably, only 6-OHDA-treated cells retain sufficient energy to execute apoptosis. On the other hand, BiP and Xbp1 mRNA did not increase significantly at any time following MPP⁺ treatment, but were induced by 6-OHDA. This might indicate that the two responses are distinct from the beginning, despite sharing common participants.

In primary cultures, the difference between 6-OHDA and MPP⁺ appears to be even more distinct. Markers of UPR seen in 6-OHDA-treated MN9D cells were also seen in 6-OHDA-treated primary cultures (Fig. 6). In contrast, MPP⁺ did not appear to up-regulate CHOP or to phosphorylate eIF2 α or c-Jun in dissociated dopaminergic neurons (Fig. 6). Further investigation will be needed to determine whether this is the result of differences between MN9D cells and primary cells, or of the manner or timing in which the cells were treated.

Unraveling the biological processes by which PD mimetics induce their neurotoxic effects is important to accurately model this disease. However, despite decades of use, the complex signaling pathways by which 6-OHDA and MPP⁺ act remain unclear. The unsuspected finding that 6-OHDA and MPP⁺ trigger components of the UPR pathway will lead to a better understanding of the application of these agents in models of nigral degeneration and improve the interpretation of the results. In addition, information obtained from 6-OHDA- or

MPP⁺-mediated cell death may also contribute toward understanding other disorders such as excitotoxicity, amyotrophic lateral sclerosis, ataxias, etc. These findings support the emerging role of ubiquitin-proteasome system dysfunction in PD, and provide a connection between oxidative stress, mitochondrial dysfunction, and impaired protein degradation.

Acknowledgments—We thank Dr. M. Watson for helpful discussions of microarray experimental design and data interpretation, as well as the Alvin J. Siteman Cancer Center at Washington University School of Medicine and Barnes-Jewish Hospital in St. Louis, Missouri, for the use of the Multiplexed Gene Analysis Core, which provided generation, hybridization, and scanning of target cRNA services. The Siteman Cancer Center is supported in part by National Institutes of Health NCI Cancer Center Support Grant P30 CA91842.

Note Added in Proof—While this manuscript was under review, Ryu *et al.* (Ryu, E. J., Harding, H. P., Angelastro, J. M., Vitolo, O. V., Ron, D., and Greene, L. A. (2002) *J. Neurosci.* 22, 10690) demonstrated induction of the unfolded protein response in 6-OHDA-treated PC12 cells and sympathetic neurons. This supports our findings in MN9D cells and primary dopaminergic cultures that 6-OHDA is an inducer of ER stress.

REFERENCES

1. Lansbury, P., and Brice, A. (2002) *Curr. Opin. Cell Biol.* 14, 653
2. Polymeropoulos, M. H., Lavedan, C., Leroy, E., Ide, S. E., Dehejia, A., Dutra, A., Pike, B., Root, H., Rubenstein, J., Boyer, R., Stenroos, E. S., Chandrasekharappa, S., Athanassiadou, A., Papapetropoulos, T., Johnson, W. G., Lazzarini, A. M., Duvoisin, R. C., Di Iorio, G., Golbe, L. I., and Nussbaum, R. L. (1997) *Science* 276, 2045–2047
3. Kreuger, R., Kuhn, W., Mueller, T., Woitalla, D., Graeber, M., Keisel, S., Przuntek, H., Epplen, J. T., Scheels, L., and Riess, O. (1998) *Nat. Genet.* 18, 106–108

4. Spillantini, M. G., Schmidt, M. L., Lee, V. M., Trojanowski, J. Q., Jakes, R., and Goedert, M. (1997) *Nature* 388, 839–840
5. Kitada, T., Asakawa, S., Hattori, N., Matsumine, H., Yamamura, Y., Minoshima, S., Yokochi, M., Mizuno, Y., and Shimizu, N. (1998) *Nature* 392, 605–608
6. Shimura, H., Hattori, N., Kubo, S., Mizuno, Y., Asakawa, S., Minoshima, S., Shimizu, N., Iwai, K., Chiba, T., Tanaka, K., and Suzuki, T. (2000) *Nat. Genet.* 25, 302–305
7. Imai, Y., Soda, M., Hatakeyama, S., Akagi, T., Hashikawa, T., Nakayama, K. I., and Takahashi, R. (2002) *Mol. Cell* 10, 55–67
8. Imai, Y., Soda, M., Inoue, H., Hattori, N., Mizuno, Y., and Takahashi, R. (2001) *Cell* 105, 891–902
9. Leroy, E., Boyer, R., Auburger, G., Leube, B., Ulm, G., Mezey, E., Harta, G., Brownstein, M. J., Jonnalagada, S., Chernova, T., Dehejia, A., Lavedan, C., Gasser, T., Steinbach, P. J., Wilkinson, K. D., and Polymeropoulos, M. H. (1998) *Nature* 395, 451–452
10. McNaught, K. S., Mytilineou, C., Jnabaptiste, R., Yabut, J., Shashidharan, P., Jennert, P., and Olanow, C. W. (2002) *J. Neurochem.* 81, 301–306
11. McNaught, K. S., Bjorklund, L. M., Belizaire, R., Isacson, O., Jenner, P., and Olanow, C. W. (2002) *Neuroreport* 13, 1437–1441
12. Stokes, A. H., Hastings, T. G., and Vrana, K. E. (1999) *J. Neurosci. Res.* 55, 659–665
13. Blum, D., Torch, S., Lambeng, N., Nissou, M., Benabid, A. L., Sadoul, R., and Verna, J. M. (2001) *Prog. Neurobiol.* 65, 135–172
14. Curtius, H. C., Wolfensberger, M., Steinmann, B., Redweik, U., and Siegfried, J. (1974) *J. Chromatogr.* 99, 529–540
15. Fornstedt, B., Rosengren, E., and Carlsson, A. (1986) *Neuropharmacology* 25, 451–454
16. Spencer, J. P., Jenner, P., Daniel, S. E., Lees, A. J., Marsden, D. C., and Halliwell, B. (1998) *J. Neurochem.* 71, 2112–2122
17. Speciale, S. (2002) *Neurotoxicol. Teratol.* 24, 607
18. Langston, J. W., Ballard, P., Tetrud, J. W., and Irwin, I. (1983) *Science* 219, 979–980
19. Beal, M. F. (2001) *Nat. Rev. Neurosci.* 2, 325–334
20. Choi, W.-S., Yoon, S.-Y., Oh, T. H., Choi, E.-J., O'Malley, K. L., and Oh, Y. J. (1999) *J. Neurosci. Res.* 57, 86–94
21. Lotharius, J., Dugan, L. L., and O'Malley, K. L. (1999) *J. Neurosci.* 19, 1284–1293
22. Oh, Y., Wong, S., Moffat, M., and O'Malley, K. L. (1995) *Neurobiol. Dis.* 2, 157–167
23. Choi, W.-S., Canzoniero, L. M. T., Sensi, S. L., O'Malley, K. L., Gwag, B. J., Seonghyang, S., Kim, J.-E., Oh, T. H., Lee, E. B., and Oh, Y. J. (1999) *Exp. Neurol.* 159, 274–282
24. Choi, H. K., Won, L. A., Kontur, P. J., Hammond, D. N., Fox, A. P., Wainer, B. H., Hoffmann, P. C., and Heller, A. (1991) *Brain Res.* 552, 67–76
25. O'Malley, K. L., Liu, J., Lotharius, J. M., and Holtz, W. A. (2003) *Neurobiol. Dis.*, in press
26. O'Malley, K. L., Mack, K. J., Gandelman, K. Y., and Todd, R. D. (1990) *Biochemistry* 29, 1367–1371
27. Fleming, J. V., Fontanier, N., Harries, D. N., and Rees, W. D. (1997) *Mol. Reprod. Dev.* 48, 310–316
28. Nicotra, A., and Parvez, S. H. (2002) *Neurotoxicol. Teratol.* 24, 599–605
29. Harris, C., Maroney, A. C., and Johnson, E. M., Jr. (2002) *J. Neurochem.* 83, 992–1001
30. Castro-Obregon, S., Del Rio, G., Chen, S. F., Swanson, R. A., Frankowski, H., Rao, R. V., Stoka, V., Vesce, S., Nicholls, D. G., and Bredesen, D. E. (2002) *Cell Death Differ.* 9, 807–817
31. Nicotra, P., Leist, M., and Manzo, L. (1999) *Trends Pharmacol. Sci.* 20, 46–51
32. Liu, C.-Y., Takemasa, A., Liles, W. C., Goodman, R. B., Jonas, M., Rosen, H., Chi, E., Winn, R. K., Harlan, J. M., and Chuang, P. I. (2003) *Blood* 101, 295–304
33. Barone, M. V., Crozat, A., Tabae, A., Philipson, L., and Ron, D. (1994) *Genes Dev.* 8, 453–464
34. Zinsner, H., Kuroda, M., Wang, X., Batchvarova, N., Lightfoot, R. T., Remotti, H., Stevens, J. L., and Ron, D. (1998) *Genes Dev.* 12, 982–995
35. Jousse, C., Bruhat, A., Harding, H. P., Ferrara, M., Ron, D., and Fournoux, P. (1999) *FEBS Lett.* 448, 211–216
36. Bertolotti, A., Zhang, Y., Hendershot, L. M., Harding, H. P., and Ron, D. (2000) *Nat. Cell Biol.* 2, 326–332
37. Urano, F., Wang, X., Bertolotti, A., Zhang, Y., Chung, P., Harding, H. P., and Ron, D. (2000) *Science* 287, 664–666
38. Leppa, S., and Bohmann, D. (1999) *Oncogene* 18, 6158–6162
39. Calton, M., Zeng, H., Urano, F., Till, J. H., Hubbard, S. R., Harding, H. P., Clark, S. G., and Ron, D. (2002) *Nature* 415, 92–96
40. Lee, K., Tirasophon, W., Shen, X., Michalak, M., Prywes, R., Okada, T., Yoshida, H., Mori, K., and Kaufman, R. J. (2002) *Genes Dev.* 16, 452–466
41. Albers, D. S., and Beal, M. F. (2000) *J. Neural Transm. Suppl.* 59, 133–154
42. Langston, J. W., and Ballard, P. A., Jr. (1983) *N. Engl. J. Med.* 309, 310
43. Hattori, N., Kitada, T., Matsumine, H., Asakawa, S., Yamamura, Y., Yoshino, H., Kobayashi, T., Yokochi, M., Wang, M., Yoritaka, A., Kondo, T., Kuzuhara, S., Nakamura, S., Shimizu, N., and Mizuno, Y. (1998) *Ann. Neurol.* 44, 935–941
44. Maraganore, D. M., Farrer, M. J., Hardy, J. A., Lincoln, S. J., McDonnell, S. K., and Rocca, W. A. (1999) *Neurology* 53, 1858–1860
45. McCullough, K. D., Martindale, J. L., Klotz, L. O., Aw, T. Y., and Holbrook, N. J. (2001) *Mol. Cell Biol.* 21, 1249–1259
46. Conn, K. J., Gao, W.-W., Ullman, M. D., McKeon-O'Malley, C., Eisenhauer, P. B., Fine, R. E., and Wells, J. M. (2002) *J. Neurosci. Res.* 68, 755–760
47. Chun, H. S., Gibson, G. E., DeGiorgio, L. A., Zhang, H., Kidd, V. J., and Son, J. H. (2001) *J. Neurochem.* 76, 1010–1021
48. Ma, Y., and Hendershot, L. M. (2001) *Cell* 107, 827–830
49. Yoneda, T., Imaizumi, K., Oono, K., Yui, D., Gomi, F., Katayama, T., and Tohyama, M. (2001) *J. Biol. Chem.* 276, 13935–13940
50. Okada, T., Yoshida, H., Akazawa, R., Negishi, M., and Mori, K. (2002) *Biochem. J.* 366, 585–594
51. Ma, Y., Brewer, J. W., Diehl, J. A., and Hendershot, L. M. (2002) *J. Mol. Biol.* 318, 1351–1365
52. Kaufman, R. J., Scheuner, D., Schroder, M., Shen, X., Lee, K., Liu, C. Y., and Arnold, S. M. (2002) *Nat. Rev. Mol. Cell Biol.* 3, 411–421
53. Williams, B. R. (2001) *Science's STKE* http://www.stke.org/cgi/content/full/OC_sigtrans;2001/89/re2
54. Mengesdorf, T., Althausen, S., and Paschen, W. (2002) *Brain Res. Mol. Brain Res.* 104, 227–239
55. Yamashita, K., Takahashi, A., Kobayashi, S., Hirata, H., Mesner, P. W., Jr., Kaufmann, S. H., Yonehara, S., Yamamoto, K., Uchiyama, T., and Sasada, M. (1999) *Blood* 93, 674–685
56. Ward, C., Chilvers, E. R., Lawson, M. F., Pryde, J. G., Fujihara, S., Farrow, S. N., Haslett, C., and Rossi, A. G. (1999) *J. Biol. Chem.* 274, 4309–4318
57. Zimmermann, K. C., Bonzon, C., and Green, D. R. (2001) *Pharmacol. Ther.* 92, 57–70
58. Wajant, H. (2002) *Science* 296, 1635–1636
59. Strasser, A., O'Connor, L., and Dixit, V. M. (2000) *Annu. Rev. Biochem.* 69, 217–245
60. Rao, R. V., Castro-Obregon, S., Frankowski, H., Schuler, M., Stoka, V., del Rio, G., Bredesen, D. E., and Ellerby, H. M. (2002) *J. Biol. Chem.* 277, 21836–21842
61. Morishima, N., Nakanishi, K., Takenouchi, H., Shibata, T., and Yasuhiko, Y. (2002) *J. Biol. Chem.* 277, 34287–34294